NOTICE

The quality of this microform is heavily dependent upon the quality of the original thesis submitted for microfilming. Every effort has been made to ensure the highest quality of reproduction possible.

If pages are missing, contact the university which granted the degree.

Some pages may have indistinct print especially if the original pages were typed with a poor typewriter ribbon or if the university sent us an inferior photocopy.

Reproduction in full or in part of this microform is governed by the Canadian Copyright Act, R.S.C. 1970, c. C-30, and subsequent amendments.

AVIS

La qualité de cette microforme dépend grandement de la qualité de la thèse soumise au microfilmage. Nous avons tout fait pour assurer une qualité supérieure de reproduction.

S'il manque des pages, veuillez communiquer avec l'université qui a conféré le grade.

La qualité d'impression de certaines pages peut laisser à désirer, surtout si les pages originales ont été dactylographiées à l'aide d'un ruban usé ou si l'université nous a fait parvenir une photocopie de qualité inférieure.

La reproduction, même partielle, de cette microforme est soumise à la Loi canadienne sur le droit d'auteur, SRC 1970, c. C-30, et ses amendements subséquents.

Canada

IDENTIFICATION OF MOLECULAR CHANGES AND VIRULENCE DETERMINANTS IN A MOUSE ADAPTED INFLUENZA VIRUS A/FM/1/47

A Thesis Submitted to the
School of Graduate Studies,
University of Ottawa

In Partial Fulfillment of the Requirements for the Degree
of
Master of Science
Department of Microbiology and Immunology
School of Medicine

By

Cecilia Smeenk

ISBN 0-612-00555-0

UNIVERSITÉ D'OTTAWA
UNIVERSITY OF OTTAWA

ABSTRACT

The human influenza virus A/FM/1/47 (FM) was mouse-adapted by serial lung passage to produce the more virulent variant A/FM/1/47-MA (FM-MA). Previous genetic analysis identified four genome segments, 4, 5, 7 and 8 that are statistically associated with virulence. The aim of this investigation was first, to find the mutations on these four genome segments and then to determine a role for these changes in disease production. Upon sequencing segments 4 and 7, single amino acid replacements were found at amino acid 47 of the HA2 subunit of the hemagglutinin (HA) and at amino acid 139 of the matrix protein (M1). Segments 5 and 8 had not mutated on mouse-adaption. Reassortant viruses of FM crossed with FM-MA, differing from each other in these single amino acid substitutions were used to determine a role for HA and M1 in viral replication kinetics and lung pathology. Previous analysis of the reassortants confirmed that segments 4 and 7 had increased virulence by $10^{2.2}$ and $10^{1.2}$ fold respectively. Viral growth kinetics were studied both in the mouse lung and in cell culture with MDCK cells. For viral pathology, standard hematoxylin, phloxine, saffron staining of formalin fixed sections, fluorescent antibody labelling of frozen sections and flow cytometric analysis for infected cells and immune cell recruitment was used to detect differences between the viruses. Although the HA has a coding change that can be observed in a functional assay of the optimum pH

of fusion and in differential cleavage with trypsin and N-chlorosuccinimide, no biological role could be found for this mutation in replication or pathology. The matrix protein however, has a role in both replication and pathology and its coding change can be observed as a shift on SDS-PAGE. It was shown that viruses containing the matrix protein of FM-MA could replicate as quickly and to as high a titer as FM-MA itself. In pathology, it was apparent that segment 7 contributes to the early onset of interstitial pneumonia and that these reassortants can infect a greater number of cells than FM or the segment 4 reassortants. The parental FM-MA strain infects more cells in the lung and is more virulent than FM X FM-MA reassortants containing segments 4 and 7, thus the unaccounted for virulence in FM-MA must be controlled by a gene(s) other than those coded for by segments 4, 5, 7 and 8.

ACKNOWLEDGEMENTS

I would like to thank Dr. E. Brown for guiding me through the many aspects of this project and enriching my scientific experience. His patience, encouragement and sense of humour was greatly appreciated.

I would also like to thank the members of my thesis advisory committee, Drs. K. Wright, E. Rossier, B. Burns and D. Franks for their generous advice and technical help.

Thanks also to the graduate students, faculty and staff who make the department a great place to work.

I am especially grateful to my family for encouraging and supporting me throughout my education.

I would finally like to express my gratitude to God who watches over all things and who is an unending source of hope and courage.

TABLE OF CONTENTS

LIST OF FIGURES

page

LIST OF TABLES

LIST OF APPENDICES

LIST OF ABBREVIATIONS

ACK	Ammonium chloride containing buffer
BSA	Bovine serum albumin
CD3	T cell marker
CD45	B cell marker
cDNA	comlementary DNA
CPE	Cytopathic effect
DEPC	Diethyl pyrocarbonate
DNA	Deoxyribonucleic acid
dNTP	Deoxyribonucleotide
DMSO	Dimethyl sulfoxide
DTT	Dithiothreitol
ELISA	Enzyme linked immunosorbant assay
FA	Fluorescent antibody
Fl1, Fl2, Fl3	Fluorescence detectors on cytometer for fluorescein, phycoerythrin and propidium iodide respectively
FITC	Fluorescein isothiocyanate
HA (0, 1, 2)	Influenza hemagglutinin protein (subunits)
HPS	Hematoxylin phloxine saffron
IL-1	Interleukin 1 (endogenous pyrogen)
M1, 2	Influenza matrix and ion channel proteins
MAb	Monoconal antibody
Mac-1	Macrophage and neutrophil marker
MDCK	Madin Darby canine kidney cells
MEM	Minimal essential medium
MMuLV RT	Moloney's murine leukemia virus reverse transcriptase

MOI	Multiplicity of infection
mRNA	Messenger RNA
NA	Influenza neuraminidase protein
NCS	N-chlorosuccinimide
NP	Influenza nucleoprotein
NS1, 2	Influenza nonstructural proteins
PA, PB1, PB2	Influenza polymerase proteins
PBS	Phosphate buffered saline
PCR	Polymerase chain reaction
PE	Phycoerythrin
PEG	Polyethylene glycol
PFU	Plaque forming units
PI	Propidium iodide
PMSF	Phenylmethylsulfonyl fluoride
PPO	Diphenyloxazole
OCT	Embedding medium for frozen tissue
RBC	Red blood cells
RER	Rough endoplasmic reticulum
RIPA	Radioimmunoprecipitation assay
RNA	Ribonucleic acid
RNP	Ribonucleoprotein
rpm	revolutions per minute
RPMI 1640	Nutrient rich cell culture medium
S400	Sephacryl 400
SDS-PAGE	Sodium dodecyl sulfate polyacrylamide electrophoresis

STE	Sodium, Tris and EDTA containing buffer
TBE	Tris, borate, EDTA containing buffer
TE	Tris and EDTA containing buffer
U	Units
VRNSD	Vanadyl ribonucleoside complex
2YT	Yeast extract, tryptone broth

INTRODUCTION

Importance of Influenza A as a Human Pathogen

The influenza virus is an important human pathogen that has been causing recognized outbreaks since at least the 16th century and perhaps for hundreds of years earlier. (Stuart-Harris et al, 1985; Kilbourne, 1987). More recently, in 1918, influenza A was responsible for the third worst pandemic in recorded history with a conservative estimate of 21 million people killed and 1 billion people attacked by the virus (Collier, 1974). Since then, there have been a number of major pandemics, notably 1946, 1957, 1968 and 1977 that coincide with the introduction of new influenza subtypes (Kilbourne, 1987). Influenza viruses are members of the family *Orthomyxoviridae*, that is divided into two genera. One genus is composed of influenza serotypes A and B and the other genus is composed of influenza serotype C along with Thogoto and Dhori viruses (Kingsbury, 1990). This thesis will be concerned with only the influenza type A virus.

The influenza virus causes an acute febrile infection after an approximately two day incubation period (Douglas, 1990; Ray, 1990). The symptoms include fever, myalgia, headache, nonproductive cough and shaking chills (Ray, 1990). Most of the symptoms usually resolve within one week, but fatigue, cough and weakness can persist an additional 2 to 3 weeks (Ray, 1990). Pneumonia, either primary viral pneumonia or bacterial superinfection of the already damaged lung, is

the most common complication of an influenza infection (Douglas, 1990). Other complications can include Reye's syndrome in children, encephalopathy, myopathy and carditis, but all of these are relatively uncommon. Influenza is typically confined to the upper respiratory tract with the occasional lower respiratory tract infection and rarely viremia (Ray, 1990).

There are three situations in which an influenza virus infection may result in death: 1. the patient has an underlying pulmonary or cardiac problem, 2. the patient develops a bacterial superinfection, or 3. the patient develops primary viral pneumonia (Ray, 1990). Currently, the usual case fatality rate is 1 in 10 000 with 80 to 90% of the deaths due to influenza occurring in those 65 years of age and older (Anderson, 1991). They are often the most vulnerable group because they have the largest incidence of underlying medical disorders (Ray, 1990). Contrasting this, in London during the 1918 pandemic, the case fatality rate for those 20-40 years of age was 50% and they represented 44% of the total influenza deaths (Stuart-Harris et al, 1985). These deaths were due to an unusually high rate of pneumonia suspected to be both of viral and bacterial superinfection in origin (Stuart-Harris et al, 1985). In the 1957 pandemic, 25% of the influenza pneumonia deaths were entirely primary viral in origin (Mims, 1976). Although currently there is antibiotic treatment for bacterial infections, there is still

little treatment for viral infections.

Prevention and Treatment

The most effective way to prevent morbidity and mortality is through vaccination. In North America, the only vaccine that has been available since the 1940s is an inactivated whole or subunit vaccine (Couch, 1993; Palache et al, 1993). This reportedly is effective in preventing illness in 25 to 95% of those vaccinated and on average can prevent infection about 70% of the time (Couch, 1993; Small, 1990; Anderson, 1991) Yearly vaccination is primarily recommended for the elderly or people with medical conditions that predispose them to complication due to influenza as well as medical personnel and others who are in close contact with those who are at high risk (Douglas, 1990). In an attempt to improve the efficacy of vaccination, a live attenuated virus vaccine produced by cold-adapting the virus has been generated and has undergone evaluation. It is hoped that this vaccine will be more effective at preventing infection since it is administered by the normal route of infection and should therefore elicit a more specific, local immune response (Couch, 1993; Douglas, 1990). This vaccine has already proven to be a superior immunogen in trials with children and should be available for general use shortly.

Apart from vaccination, there is also the antiviral agent amantadine that can be used in the prevention and treatment of influenza A infections. It was found to be safe for a 6

week prophylaxis period and effective at preventing illness in 70% of the people tested who had no prior antibodies to the virus. (Monto and Arden, 1992). Also, if amantadine is given within 24 hours of symptoms, it is capable of reducing the duration and symptoms of the infection by one to two days (Douglas, 1990). However, there are the problems of side effects (especially in the elderly) and viral resistance associated with the use of amantadine, so it is used with caution in only specific situations (Monto and Arden, 1992).

Viral Hosts

Influenza A infects humans and a variety of animals including waterfowl, pigs, poultry, horses, seals, mink, and whales (Webster et al, 1992). Influenza infection in some of these animals is important in that they are significant sources of income to farmers and livestock breeders. These animals are also important in that they constitute a potential reservoir from which novel virus strains may be introduced to the human population. The major participants in this cycle are believed to be the aquatic birds, pigs and possibly horses (Webster et al, 1992). Aquatic birds are speculated to be the source of all influenza viruses in other species. (Webster et al, 1992). From evolutionary studies of viruses, investigators have traced genes of avian origin in the human pandemic strains (Webster et al, 1992). They have also discovered that genetic reassortment is taking place between avian-like viruses and human-like viruses in pigs and

that periodically, humans and swine transmit influenza to each other (Webster et al, 1992; Webster et al, 1993). The genes of one virus may have different origins because influenza has a segmented genome that is readily amenable to reassortment during coinfection of the same host.

Genes and Proteins

Influenza A is a negative sense singled stranded RNA virus with 8 segments encoding 10 known proteins (Lamb, 1989). Figure 1 is a schematic diagram the influenza virus with its host-derived lipid envelope and antigenic hemagglutinin (HA) and neuraminidase (NA) protein spikes on the outside and the internal matrix (M1), polymerase (PB1,PB2 and PA) and nucleoprotein (NP) enclosed with the RNA strands.

Of the eight RNA segments, the largest 3 code for the polymerase proteins PB1, PB2 and PA. These form a complex which binds to 7-methylguanosine caps of host RNA polymerase II transcripts and use them along with the first 10-13 nucleotides to prime viral transcription. They then go on to complete transcription and poly A addition (Lamb, 1989).

RNA segment 4 codes for the viral hemagglutinin which is one of the two glycoprotein spikes found on the surface of the virus. As is the general rule for glycoproteins, HA or a full length precursor (HA0) is synthesized in the rough endoplasmic reticulum (RER) and is transported and glycosylated through the Golgi network whereupon it migrates to the cell membrane to be inserted as trimers on viral

Figure 1: Schematic Diagram of Influenza A Virion Structure

(Taken from Kingsbury, 1990) PB2, PB1 and PA - polymerase complex proteins; HA - hemagglutinin protein; NP - nucleoprotein; NA - neuraminidase protein; M1 - matrix protein; M2 - ion channel protein; NS1 and NS2 - non structural proteins

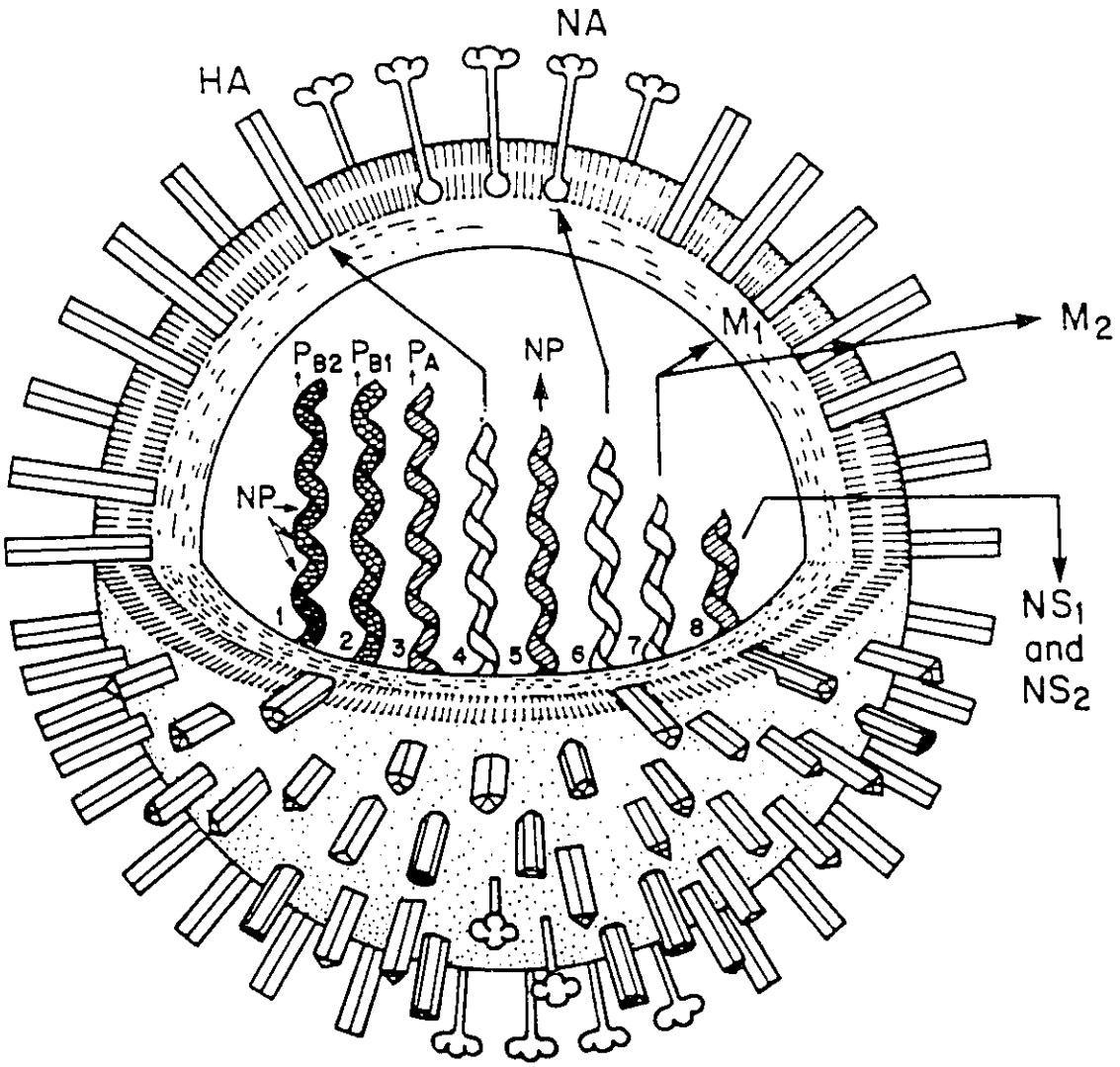
NA
HA
M1
M2
PB2
PB1
PA
NP
NP
1
2
3
4
5
6
7
8
NS1
and
NS2

assembly (Lamb, 1989). In order to be infectious, HA0 must be proteolytically cleaved into two subunits, HA1 and HA2 either by an intracellular or extracellular trypsin-like protease (Bosch et al, 1981; Kido et al, 1993). The HA1 and HA2 subunits remain joined through disulfide bonding and are folded such that HA1 makes up the globular head region where many of the antigenic changes take place and HA2 which makes up the stalk region anchoring the protein in place with its transmembrane region (Webster et al, 1992).

HA has more than one function in the life cycle of the influenza virus. Initially, it serves as a receptor to bind sialic residues on the host cell (Wiley and Skehel, 1987). After binding and being endocytosed by the host cell, the HA encounters a drop in pH within the endosome (Marsh and Helenius, 1989; Carr and Kim, 1993). This pH change results in a conformational change in the HA, exposing the fusion peptide (HA2 a.a. 1-25) that will act in membrane fusion with the endosomal membrane allowing the release of viral contents into the cytoplasm (Marsh and Helenius, 1989). It is believed that the HA2 has two important roles in these events. First, it has a loop region (HA2 a.a. 54-81) that is thought to become a coiled coil with a drop in pH and by coiling, it will reorient the fusion peptide from the direction of the viral membrane toward the globular head region of the protein (Carr and Kim, 1993). The second role of the HA depends on its transmembrane region which has

proven to be important in achieving complete fusion of the virus with the endosomal membrane (Kemble et al, 1994).

In type A influenza virus, there are 14 subtypes of HA, of which only the first three have been found in human strains while all of them are found in avian strains (Webster et al, 1993). A change in subtype constitutes an antigenic "shift" and is often responsible for producing pandemics (Taylor, 1993). HA mutations within one subtype result in antigenic "drift" and could be responsible for epidemics in interpandemic periods (Stuart-Harris, 1985). In humans, usually only one subtype is dominant in a given year (Couch, 1993).

Segment 5 encodes the nucleocapsid protein which is the second most abundant viral protein (Lamb, 1989). Its major function is to bind RNA to form the ribonucleoprotein (RNP), the template for transcription, allowing RNA synthesis and elongation to proceed (Lamb, 1989).

Segment 6 RNA codes for the other viral spike protein, the neuraminidase. The NA spike is a homotetramer that, like the HA, has a stalk region and a globular head region. Its primary function is to cleave terminal sialic acids (Lamb, 1989). This may either help the virus find target cells in a sialic acid rich mucin coating the respiratory tract or function in releasing the newly budded virus from the infected cell (Lamb, 1989). It is primarily this enzymatic function and the fact that the substrate is known that has

made the NA the subject of rational drug design. Using the 3-D structure of NA derived from X-ray crystallography investigators have searched for an analog to sialic acid that would bind tightly to the active site causing the NA to be incapable of carrying out its normal functions and rendering the virus impotent (von Itzstein et al, 1993). Segment 6 protein, like the HA is a major antigenic determinant of the virus and has 9 subtypes of which only the first two have been found in human strains (Webster et al, 1992).

The smallest RNA segments, 7 and 8, code for 4 proteins. The M1 and NS1 proteins encoded by full length transcripts of segments 7 and 8 respectively and are not spliced whereas M2 and NS2 are encoded by spliced messenger RNA (mRNA) derived from these segments (Lamb, 1989).

Segment 7 codes for the matrix protein which is the most abundant protein in the virion, lining the inside of the viral envelope. Its most obvious role is providing structural integrity to the virion but it seems that it has more than just this one function. By monoclonal antibody mapping of the protein, a functional map was compiled by Herlocher et al in 1992 and may be found in Figure 3 in the results section. On this map the lipid binding, RNA binding, and transcription inhibiting areas are indicated, locating regions involved in these functions. Once again by using antibodies, it was discovered that M1 protein is important in chaperoning the export of newly synthesized viral RNPs from

the nucleus to the cytoplasm (Martin and Helenius, 1991). In contrast to this, during the initial entry of the viral contents to the cytoplasm, the M1 must dissociate from the RNPs so that they can reach the nucleus for replication. It has been suggested that the pH drop that induces HA mediated viral fusion is also instrumental in dissociating M1 from the RNP (Helenius 1992). M2 protein has also been connected to these events (Helenius, 1992). M2 is the other protein coded for by segment 7. It shares only 9 N terminal amino acids with M1 while the rest is encoded by a second partially overlapping reading frame (Lamb, 1989). Although only 97 amino acids in length, M2 plays several key roles in viral uncoating, viral protein maturation and amantadine resistance. By testing electrical current changes on frog oocytes expressing M2, Pinto et al (1992) found that the M2 protein has ion channel activity. This activity is important for virus uncoating through M1 dissociation in that the M2 channels allow H+ to enter the virion thus resulting in a drop in pH, releasing the M1 protein from RNP (Helenius, 1992). In protein maturation, the M2 tetramer form channels in the Golgi to allow H+ to escape and thus prevent the maturing HA protein of some influenza strains from irreversibly entering the low pH fusion form (Takeuchi and Lamb, 1994). Virions containing the low pH form of HA are non-infectious because they have lost receptor binding ability. M2 is the usual target of amantadine. Amantadine

blocks the ion channel formed by M2 so that it can no longer regulate the pH in different parts of the infected cells. In amantadine resistance, it is commonly the M2 that has mutated, making it no longer susceptible to blockage by the antiviral agent (Holsinger et al, 1994).

The smallest RNA segment to be considered is segment 8 coding for the two nonstructural proteins (NS1, 2) (Lamb, 1989). NS1 is located abundantly throughout the infected cell and was demonstrated to have viral RNA (vRNA) binding capacity by Hatada et al (1992). More recently it was found to have a role in the stimulation of translation of M1 and perhaps other late proteins such as NP and NA (Enami et al, 1994). Recent evidence also shows that NS2 may be a structural component of virions as shown by specific immune precipitation of NS2 from virions (Richardson and Akkina, 1991).

Replication

The first step in replication that must be accomplished is the viral attachment and entry into the host cell. Viral HA is involved in binding to cell surface glycoproteins with terminal sialic acids (Couceiro et al, 1993). Hemagglutinins from different influenza viruses differ in their receptor specificity and can recognize the various linkages of sialic acid found in nature (Couceiro et al, 1992; Higa et al, 1985). A good example of this recognition of sialic acid in different linkages with galactose is that the avian and human

strains of influenza were found to have different specificities (Couceiro et al, 1992). With the viral HA bound to a cell, the next step is internalization by receptor mediated endocytosis (Marsh and Helenius, 1989). Once the virus is in the endosome, the pH within the endosome drops and results in the conformational change in the HA, exposing the fusion peptide (Kemble et al, 1994). At the same time, M2 ion channels in the virion allow for the internal acidification of the virus and when the viral contents enter the cytoplasm with the HA mediated membrane fusion, the M1 has been loosened from the viral RNP so that the RNP may proceed to the nucleus for further replication steps (Helenius, 1992). Once the RNPs have gone to the nucleus, primary transcription of mRNAs begins. For mRNAs to be transcribed, the viral polymerase complex composed of proteins PB1, PB2 and PA must steal 7-methylguanosine caps from the recently transcribed host mRNAs (Krug et al, 1989). Without these caps, the host mRNAs are destabilized and are quickly degraded, thus preventing newly made cellular mRNA from reaching the cytoplasm for translation (Katze and Krug, 1990). Also, in the cytoplasm, viral mRNAs are being translated into proteins while pre-existing cellular mRNA are inhibited (Katze and Krug, 1990). When there is enough newly made NP returning to the nucleus after translation in the cytoplasm, vRNA replication is triggered (Krug et al, 1989). Synthesis begins from the input vRNA template to

produce complementary RNA (cRNA) that is then copied into nascent vRNA. While the new vRNA is being transcribed, the NP encapsidates the RNA (Krug, 1989). By this time, late M1 synthesis has taken place and it can bind and escort the new viral RNPs from the nucleus to the cytoplasm where assembly can take place (Martin and Helenius, 1991). Assembly is thought to involve transmembrane interactions of M1 with the HA and NA glycoproteins which have inserted in the host cell membrane after processing in the Golgi (Kilbourne, 1987). With the M1 binding both the RNPs and the glycoproteins in the membrane it is proposed that a bulge in the plasma membrane around the nucleocapsid forms, producing the virion particle through a budding process. The neuraminidase is believed to be important for the final release of the virus from the surface of the host cell since it removes sialic acid receptors from the plasma membrane (Kilbourne, 1987).

Virulence Factors

Virulence or pathogenicity is the ability of a microorganism to cause damage and disease in the host (Mims, 1987). This definition is best understood by a description of the viral virulence attributes. The main aspects of microbial pathogenicity as described by Sweet and Smith (1980) are the following : mucous surface interaction, entry to host tissues, replication *in vivo*, interference with host defenses, spread from initial site of replication, damage to host and tissue and host specificity. They also state that in

discovering which of the microbial or host characteristics are responsible for these virulence determinants, three objectives must be satisfied. These include: finding a method for identifying and comparing high and low virulent strains, comparing the strains in tests to measure their pathogenicity according to the virulence determinants listed above and lastly, identifying the biochemical basis for the virulence differences.

Many investigators attempting to determine the virulence factors of influenza A used mutants. These mutants, whether derived from cold-adaption, mouse-adaption or neuroadaption allowed a comparison of the original non-adapted virus with the adapted virus. Alternatively, by studying mutants with some similar properties they could look for common attributes rather than changes.

The first two criteria from the Sweet and Smith list for finding virulence factors, namely the identification and measurement of pathogenicity have historically been easier to fulfil than the third, identification of biochemical changes. For example, Hirst in 1947 had passaged a virus in mouse lung that consequently increased the ability of this new strain to kill its mouse host. He could measure the amount of viral replication and changes in antigenic pattern, but at that time he had no way of determining the changes that had actually occurred in the virus to account for the virulence difference.

With the development of genetic analysis and the ability to follow gene reassortment and mutations, all of the genes of influenza have been shown to be determinants of virulence. Changes in PB1 and PB2 are believed to contribute to the cold-adapted (attenuated) human influenza phenotype (Herlocher et al, 1993) and a PA mutant has been associated with a change in host range restriction by Almond (1977) in a fowl plague virus. Mutations in HA, segment 4 change host range, cleavability or receptor specificity and have been correlated with changes in virulence in both avian and human viruses (Webster et al, 1986; Katz and Webster, 1992; Webster and Rott, 1987; Couceiro et al, 1993). Segment 5 is possibly involved in attenuation of the cold adapted virus (Herlocher et al, 1993). NA is involved in mouse neurovirulence (tissue specificity) with the loss or gain of a glycosylation site being of special importance (Ward et al, 1994; Li et al, 1993; Sugiura and Ueda, 1980). Sugiura and Ueda (1980) have also found M and NS to be important secondary determinants of neurovirulence. Herlocher et al (1993) reported that M1 was important in cold-adaption while it has also been found to carry mutations in high yield viruses (Baez et al, 1980). The problem with some of these reports is exemplified by some of the work done on cold-adapted viruses. Klimov et al (1992) and Cox et al (1988) reported 8 and 11 amino acid changes respectively in their cold-adapted virus strains with the involvement of nearly every gene. Whereas these studies

identify specific genes with virulence, it is difficult to determine the specific functions of these genes in virulence since more than one gene has mutated on adaption, thus preventing the linking of individual genes with individual function. A further difficulty in deciphering these results lies in the fact that many of these changes probably arose strictly through the passaging of the virus and are not necessarily important to the attenuation phenotype. In recent years, a technique has been developed that can reintroduce a foreign gene into the influenza virus, so that known mutations artificially produced by site directed mutagenesis may be tested for virulence on a standardized background (Luytjes et al, 1989). Accordingly, a mutation that is thought to be important in viral pathogenesis can be produced and reintroduced into the virus to see if indeed this is the case.

It is obvious from the preceding list of virulence determinants associated with specific gene segments, that no one gene determines virulence. Actually, it is well recognized that virulence is a multifactorial process (Webster et al, 1993). Often a combination of factors is required in order to express the elevated virulence. If one factor is missing, or if one factor is added to a pre-existing complementary set, the result can be an attenuated virus or enhanced virulence. These "constellation effects" of genes are illustrated by work from Scholtissek's

laboratory (1977), where crossing two avirulent parents resulted in virulent reassorted progeny and where transfer of one or more genes from a particular avirulent strain was all that was required to make another avirulent strain pathogenic. Conversely, avirulent reassortants can be derived from 2 virulent parental strains. Thus it has been concluded that there is an optimum constellation of genetic determinants that is required for virulence. Finding out the role of individual genes operating in the control of virulence is a challenge due to the problem of this gene interaction. In the present study, all mutated genes are analyzed on the same genetic background to avoid gene interaction that occurs in the reassortment of genes derived from different influenza virus strains.

Influenza Immunology

Apart from the factors introduced by the genes of the virus itself in an infection, the host contribution in infection must also be considered. One of the virulence determinants included overcoming host immune defenses. There are two aspects of the immune system that can have an influence on the virulence of an influenza infection. First, the immune system works to protect the host from a widespread infection through phagocytosis, cellular cytotoxicity and antibody production (Small, 1990; Anderson, 1991). Alternatively, the immune system can be involved in exacerbating the lung pathology in an overzealous reaction to

infection (Wyde et al, 1977; Wyde and Cate, 1978; Peterhans et al, 1988).

In the protection against influenza infection, neutrophils are the first line of defense (Hartshorn et al, 1990). This is a non-specific type of interaction whereby the immune cell adheres to infected cells and produces reactive oxygen species that kill cells (Tait et al, 1993). Neutrophils are also critical for the recruitment of macrophages and lymphocytes (Tait, 1993). When the macrophages are recruited to the site of infection, they help in phagocytosing debris as well as assisting in antigen presentation for the specific immune response which is coordinated by the T cells (Johnston, 1988). Cytotoxic T cells are very important for influenza virus clearance (Hennet et al, 1992). They function to destroy antigen bearing cells and in so doing, aid in recovery. They tend to target internal virus determinants which are often more cross reactive between different virus strains than the external determinants which are under a different immune selection pressure (Kees and Krammer, 1984). B cells produce anti-HA and NA antibodies that will speed viral containment as well as aid in the prevention of subsequent reinfection (Kees and Krammer, 1984; Small, 1990). Because of frequent shift and drift in influenza virus glycoproteins HA and NA, the virus often can evade the humoral responses in previously infected individuals.

Contrary to the host protective design of the immune system, there is evidence that it can also enhance the pathology of an influenza A virus infection. The neutrophils, being somewhat non-specific and producing oxygen radicals, can damage uninfected cells (Peterhans et al, 1988). They can also be triggered to degranulate, releasing cathepsins, peroxidase, phosphatases, and other potentially destructive enzymes (Tate and Repine, 1983). The macrophages next recruited to the site may become infected with influenza and apart from possibly aiding in spread of the virus, the macrophage could also become disabled because of their susceptiblity to infection (Bender et al, 1993). Macrophages also produce endogenous pyrogen (IL-1) which can contribute to the overall toxicity of influenza infection. Even killed virus, introduced into the bloodstream of laboratory animals can result in fever, edema, hemorrhage and death. This is attributable to IL-1 production and possibly the generation of reactive oxygen species along with its related pathways (Peterhans et al, 1988). T cells are also involved in some pathology as is shown by work with nude mice. When the nude mice were given lethal doses of influenza virus, they tended to live longer and with less lung pathology than those mice with T cells (Wyde et al, 1977). The nude mice do eventually die of a persistent infection that often spreads from the lungs to produce encephalitis. So, although the T cells are needed to clear and contain the infection, their response

appears to also add to the damage induced by the infection.

Animal Models

Having already cited examples of experiments where animal models are used, a description of the two most commonly used models should be included. Depending on the type of study, either ferrets or mice are frequently used.

Ferrets used in influenza A infection demonstrate a very similar pattern of disease symptoms to that of human infection. The infection is generally confined to the upper respiratory tract, with fever and some lung involvement. The virulence that is shown by a virus in ferret infections generally correlates well with the virulence that would be experienced in a human infection with the same virus (Sweet and Smith, 1980).

With mice, the pattern of disease is somewhat different. Human viruses although capable of reproducing in mouse respiratory tissue generally do not cause disease. After the virus has been serially passaged through mouse lung it can become virulent. Not all viral strains can be adapted in this way, possibly due to a prohibitive number of changes to become virulent (Hirst, 1947). Typically, infection is established in mice by intranasal installation of a virus suspension while lightly anesthetized to allow the inoculum to enter the lung. This method of infection effectively reproduces the same pattern of disease as a small droplet infection (Larson et al, 1976). Although correlation of the

pathogenicity of a virus in mouse lung and that of human infection is weak, the mouse model is still a valuable tool for studying primary viral pneumonia due to mouse-adapted strains (Sweet and Smith, 1980). While human and ferret infections are usually limited to the upper respiratory tract, in mice the infection predominantly takes place in the lung causing an interstitial pneumonia much like the viral pneumonia experienced in humans (Hers et al, 1962). From mouse lung lavage experiments, it was determined that the predominant immune cell type protecting uninfected lungs are alveolar macrophages. When the lungs are infected, there is an early recruitment of neutrophils along with steadily increasing numbers of macrophages and lymphocytes (Wyde and Cate, 1978).

Thesis Objectives

Background on the A/FM/1/47-Mouse Adapted Strain used to Study Influenza Virulence

The subject of this investigation is a mouse adapted variant of the human influenza A virus A/FM/1/47. It was passaged 12 times in mouse lung to produce the mouse adapted strain FM-MA with a $10^{4.3}$ fold increased ability to kill its mouse host. The aim of this investigation is to compare the two viruses to find the virulence determinants responsible for the large increase in virulence following mouse adaption.

From previous work by Brown (1990) it was discovered that segments 4, 5, 7 and 8 of the mouse adapted virus were statistically associated with increased virulence.

Reassortant viruses containing these segments from FM-MA on an FM background were also available so that the properties of each gene in virulence could be measured and characterized. For the work in the present investigation, cDNA clones of these four segments were available for both viruses. In addition to the genetic analysis of virulence that identified 4 genome segments with virulence (4, 5, 7 and 8), mutations were detected in the M1 (segment 7) and NA (segment 6) proteins of FM-MA by change in electrophoretic mobility of these proteins. In order to identify the biochemical changes in the virus, sequencing the cDNA would determine coding changes between the two genomes that has occurred upon adaptation. On the basis of genetic changes in specific genes, further standard characterization will be made of the proteins encoded by these genes. The other objective is to characterize the biological changes due to these mutations that control virulence. Some of the virulence determinants listed earlier that will be studied include the replicative capability of the viruses, damage to the host and tissue specificity as well as the possible interference of the virus with the immune system.

The study of viral growth kinetics was conducted both *in vivo* and *in vitro* so that the influence of the immune system or other host controlled barrier to replication could be observed. Viral replication could be a virulence determinant if increased replication results in more damage

to normal cellular functions and thus greater morbidity and mortality. It is not always the case that increased replication leads to greater pathology. This is described by Hirst in 1947 and indicates that pathology is not solely controlled by the extent of viral replication.

To study the pathology and tissue specificity of infected lungs, lung sections were hematoxylin, phloxine, saffron (HPS) stained or labelled with fluorescent antibodies (FA) to assess inflammatory changes as well as the extent and location of viral infection. As a further method for studying the extent of viral infection and inflammation in the lung, single cell suspensions were produced and analyzed by flow cytometry. Because multiple variables can be measured quantitatively using a variety of fluorochrome conjugated antibodies on a large number of cells in each sample, flow cytometry is a powerful technique.

Objectives

1) The first objective is **the identification of the sequence changes in segments 4, 5, 7 and 8** of FM and FM-MA, since these are the segments associated with virulence. These changes would then be the focus of attempts to determine their roles in controlling virulence.

2) Through the use of single gene reassortants, a role in **biological function of individual genes will be investigated** by studying growth kinetics, pathology and flow cytometric evaluation of the virally infected mouse lungs.

MATERIALS AND METHODS

For the components and method of preparation of all solutions and reagents please refer to Appendix I.

Viruses

The viruses used in this study were A/FM/1/47 (FM) and the mouse adapted A/FM/1/47-MA (FM-MA) produced by 12 serial mouse lung passages of FM. Reassortants were also used that contained segments 4, 4 and 7, and 4, 7 and 8 of FM-MA on a FM background. (See Table 1) The reassortants J41, W29 and TSR17 were produced by backcrossing FM x HK with FM-MA x HK reassortants in previous studies (Brown, 1990).

Table 1: Origin of Segments and Virulence of Viruses

VIRUS	ORIGIN OF SEGMENTS[a]								LD_{50} (log_{10})	INCREASE IN VIRULENCE (log_{10})
	1	2	3	4	5	6	7	8		
FM	F	F	F	F	F	F	F	F	6.5	--
FM-MA	f	f	f	f	f	f	f	f	2.2	4.3
J41	F	F	F	f	F	F	F	F	4.3	2.2
W29	F	F	F	f	F	F	f	F	3.1	3.4
TSR17	F	F	F	f	F	F	f	f	3.5	3.0

[a]FM and FM-MA segments are indicated in uppercase and lower case, respectively.

These plaque purified viruses were grown in the allantois of 10 or 11 day incubated fertile chicken eggs for 2 days at 33°C. The allantoic fluid was then collected into chilled centrifuge bottles where the debris and red blood cells

(RBCs) could be spun out at 3000 rpm for 15 min. The clarified allantoic fluid containing virus was stored at -70°C.

Plaque Assay for Quantitation of Virus

Monolayer cultures of Madin Darby Canine Kidney (MDCK) cells were used for plaque assay. Cells were grown in minimum essential medium (MEM) supplemented with 5% newborn calf serum, penicillin (100 U/ml) and streptomycin (100 µl/ml). Confluent monolayers of MDCK cells in 6 well plates, growing at 37°C in a CO_2 incubator, were used to detect viral plaque forming units (pfu). Virus was serially diluted in cold phosphate buffered saline (PBS) containing 0.2% gelatin. The monolayers were washed twice with warmed PBS then inoculated with 0.1 ml of the diluted virus in duplicate for each dilution. After a 0.5 hr adsorption of virus at 37°C, 2.5 ml of warm overlay containing medium 199 supplemented to contain 0.2% bovine serum albumin (BSA), 100 µg/ml DEAE dextran, 0.5% Oxoid agar No. 28, 1 µg/ml trypsin, 100 µg/ml streptomycin, 100 U/ml penicillin, 2.2 mg/ml sodium bicarbonate and 0.2% glucose was added to each well and allowed to solidify at room temperature. The plates were then incubated at 37°C for approximately 1½ days. At this time, the plaques were fixed with Carnoy's fixative for 20 min, the overlay washed off and the plates allowed to dry for counting.

Mice

The mice used for all virus work were 4 week old outbred

Swiss Webster(CD-1) from Charles River Laboratories. Balb/c mice, also from Charles River, were used for ascites production in the growth of hybridoma cells.

Sequencing

For details on sequencing and polymerase chain reaction (PCR) primers please see Appendix II.

cDNA Clones: Full length clones of segment 4, 5, 7, and 8 for FM and FM-MA were provided to me for sequencing. They had been produced by reverse transcription of viral RNA followed by second strand synthesis with the Klenow fragment of DNA POL I using end specific primers (Smeenk and Brown, 1994). Segments 4, 5, 7 and 8 from FM and FM-MA were sequenced using a Sequenase kit (USB) or a Pharmacia sequencing kit. These kits are based on the dideoxy chain termination method of Sanger (1977). The plasmid DNA was purified using a QIAGEN kit for midi preps after growing the culture overnight in 2YT broth at 37°C with vigorous shaking. Sequence reactions were run on a 0.2 mm thick 6% acrylamide gel with 40% urea. Running time for the gel at 50 watts using TBE buffer was approximately 6 hr for long fragments and 1 hr 45 min (until the bromphenol dye ran off) for the smaller fragments. The gel was left on the smaller glass plate for fixation, drying and exposure to film.

RNA: Any sequence differences noted in the cDNA clones were checked by direct RNA sequencing using the ^{32}P labelled primer method of Gleibter (1987). The RNA was extracted

from egg grown virus that had been precipitated with 8% (w/v) polyethylene glycol (PEG) 6000. After being shaken at 4°C for 1 hr, the PEG precipitate was harvested by centrifugation at 7000 rpm for 20 min, then resuspended in PBS. This virus concentrate, resuspended in PBS, was further purified on a 30, 45, 60% sucrose step gradient that was spun at 24 krpm for 3 hours. The interface band between the 45 and 60% sucrose was then removed with a 22 gauge needle. The virus was then diluted and pelleted at 24 krpm for 1.5 hr. This pellet was resuspended in STE buffer with 10 mM vanadyl ribonucleoside complex (VRNSD) and 0.1 mg/ml protease K added subsequently. To this mixture, a tenth volume of 10% sodium dodecyl sulfate (SDS) was added then incubated at 37°C for 30 min. Following this, the solution was phenol:chloroform (1:1) extracted twice with 5 min centrifugation at 2.5 krpm after each extraction. All of the chloroform contained isoamyl alcohol (24:1). The final extraction was chloroform, followed by overnight precipitation of the RNA at -20°C in 250 mM sodium acetate and 2.5 volumes of ethanol. To collect the precipitated RNA, it was spun at 10 krpm for 20 min, drained and washed with 70% ethanol and then dried under vacuum in a rotary evaporation Speed Vac. The resulting pellet was resuspended in 2% diethyl pyrocarbonate (DEPC) treated water for quantitation with a spectrophotometer ($1\ OD_{260} = 40\ \mu g/ml$) and subsequently stored in 3 volumes of ethanol at -70°C.

PCR Products: RNA was prepared as described above. For reverse transcription, to make cDNA, 0.2 μg of RNA was mixed with 10 mM dithiothreitol (DTT), 2.5 ng primer, 1 mM each dNTP, BRL RT buffer and 5000 U of Moloney's murine leukemia virus reverse transcriptase (MMuLV RT) in a 40 μl reaction volume and allowed to incubate at 37°C for 1 hr. For the PCR reaction, 0.5 μl of the cDNA mixture was added to 250 ng of each of two primers, PCR buffer, 0.2 mM of each dNTP and 2.5 units of Taq polymerase in 100 μl final reaction volume overlaid with sterile mineral oil. The PCR conditions were one cycle of 94°C for 5 min; 30 cycles of 1 min at 94°C, 1 min at 48°C, 2 min at 72°C; and 1 cycle of 72°C for 7 min. If there was any difficulty in obtaining PCR products from this protocol, the original RNA was further purified on a sephacryl 400 (S400) column before retrying the reactions or, alternatively, the annealing temperature of the first of the 30 cycles of the PCR reaction was reduced to 32°C from 48°C. For S400 cleaning of samples, the beads were packed in a 1 ml syringe that was plugged with siliconized glass wool and filter. A volume of TE, the same as the sample size was centrifuged at 1450 rpm for 4 min in an IEC centrifuge. The sample was then added to the syringe and collected in a fresh tube in the same manner. This method was also initially used to remove primers from PCR products prior to sequencing them. Another method for the separation of PCR products from primers was elution of the DNA band from 1% agarose gel

slices by centrifugation of the gel through a filter plugged eppendorf with a pinhole in the bottom. A final method used to remove primers from the PCR products was a commercially available "Nanospin" ultrafiltration membrane from Gelman. In this method, the reaction mixture is loaded onto the membrane with a 30 000 MW pore size, spun at 5 krpm for 15 min in a microfuge and washed 4 times with 300 µl water to leave only the large PCR product on the filter where it can be collected and used for sequence reactions. Once again, a DNA sequencing kit was used to sequence the products, but in this case, there were some alterations in the recommended method. An initial denaturation step was no longer used and in the modified denaturing/annealing step 1 µl of dimethyl sulfoxide (DMSO) was added as recommended by Winship, 1989. This denaturing/annealing mixture was boiled for 3 min then snap frozen on dry ice before proceeding with the rest of the protocol as directed by the manufacturer. The sequencing products were run identically to those described earlier.

Proteolysis of HA2 with N-chlorosuccinimide NCS

Protein Labelling: Monolayers of MDCK cells were grown in 60 mm cell culture dishes. The culture medium was drained from the dishes and they were washed twice with 37°C PBS. Following this, virus was added at an multiplicity of infection (MOI) of 5 in 0.1 ml of PBS and allowed to adsorb for 1 hr. The dishes were then overlaid with MEM supplemented with 0.2% BSA, 1 µg/ml trypsin, 100 µg/ml

streptomycin and 100 U/ml penicillin. When the overlay had been incubated for 6 hr it was removed and washed off twice with warmed PBS. At this time, 1 ml of methionine free MEM with 80 μCi/ml ^{35}S-L-methionine was added to the infected cells in each dish and incubated at 37°C for 2 hr.

Radioimmunoprecipitation of HA (RIPA): The medium was then decanted and 0.5 ml of RIPA lysis buffer with 1 mM phenylmethylsulfonyl fluoride (PMSF) was added 20 min before the cells were scraped up. The debris was removed in a 2 min at 12 krpm microfuge. The supernatant was added to 600 μl of a 20 mg/ml slurry of protein A sepharose beads and 15 μl of HA specific monoclonal antibody (MAb) with mixing overnight. The beads were washed five times with RIPA wash buffer and once with TE buffer. The beads were finally suspended in TE. For a summary of monoclonal antibody preparation, please see Appendix IV.

Cleavage of HA0 into HA1 and HA2: The immunoprecipitated HA bound to the protein A Sepharose beads was trypsinized for 20 min with 1 μg/ml trypsin in a 37°C waterbath then quenched with 1 mM PMSF. The products were run on a 12.5% Laemmli style SDS-PAGE with a stacking gel after adding sample buffer and boiling the samples for 2 min. The gel was run at 150 V constant voltage using tank buffer until the dye front left the gel. The gel was dried onto 3MM paper without prior fixing and then applied to X-OMAT XAR 5 film overnight.

NCS Cleavage of HA2: The lower HA2 band was cut out from the

gel using the film as a guide for the cutting. The protein was electroeluted into dialysis tubing in tank buffer overnight at 100 V constant voltage. The radioactivity of the dialysate was determined by scintillation counting, then concentrated by freeze drying overnight. The samples were then resuspended in a small amount of water, divided into two aliquots and acetic acid added to 0.5 M and NCS, recrystallized by ethyl acetate, at concentrations of 15 mM and 1.5 mM in the separate aliquots. The NCS cleavage took place at room temperature for 2 hr with shaking. The protein fragments were then precipitated with 5 volumes of acetone using 30 μg of BSA as a carrier. This precipitate was pelleted a 9 krpm for 20 min, rinsed with acetone, pelleted again and dried. The dried protein was resuspended in sample buffer lacking SDS, boiled for 2 min and loaded on a 17.5% Laemmli SDS-PAGE. Horse cytochrome c (MW 12 384), ß-lactoglobulin (MW 18 360) and whale myoglobin (MW 17 816) were run at the same time as markers to be stained separately with Coomassie blue. The gel was run at 160 V constant voltage until the dye front exited the gel.

Fluorography: The finished gel was fixed overnight then rinsed with methanol before soaking in DMSO for 2 hr with 1 change. The gel was then transferred to DMSO with 22% diphenyloxazole (PPO) for three hours followed by a 1 hr precipitation in water. The final incubation of the gel was in water with 3% glycerol. After this, the gel was dried and

exposed to film at -70°C for 10 weeks to detect the banding pattern.

pH of Fusion

Hemagglutination Assay (HA): In order to determine the HA titer of a virus stock, serial two fold dilution of the virus was carried out with PBS in a 96 well round bottom microtiter plate. To this, an equal volume of 0.5% washed erythrocytes was added and the whole assay was allowed to incubate at room temperature until the blood settled into round buttons in the control wells. The reciprocal of the last dilution that agglutinates the red blood cells is the HA titer.

Washing Blood: Fresh blood was added to an approximately equal volume of Alsever's solution, mixed and centrifuged at 2 krpm for 5 min. The supernatant and the buffy coat on top of the packed RBCs were removed and the cells washed in a similar manner with PBS until the supernatant remained colourless. The packed volume of cells was then diluted to the necessary concentration for HA or hemolysis assays. Cells were stored at 4°C.

Hemolysis Assay: In round bottom 96 well microtiter plates, 25 μl of virus (HA 640) was preadsorbed at 4°C for 10 min with 50 μl of 2% washed human blood that was not more than 2 days old. The supernatant was removed after centrifuging the plate at 1000 rpm for 2 min and then replaced with 75 μl of citrate buffer with 0.1 pH increments from 4.9 to 6.0. This was well mixed and incubated at 37°C for 1 hr after which it

was centrifuged once again at 1000 rpm for 2 min. The supernatant was transferred to flat bottom enzyme linked immunosorbant assay (ELISA) plates for reading of OD_{540} values in a platereader.

Viral Growth Kinetics

Mouse Lung: Mice were inoculated with 5 x 10^3 pfu of virus in 50 μl of PBS containing 0.2% gelatin while lightly anesthetized with halothane. The lungs of 3 mice for each virus at each time point were collected into 3 ml of PBS with 0.2% gelatin after euthanizing them with a 90% CO_2 10% O_2 mixture. The time points were days 0, 1, 2, 3, 5 and 7. The lungs were stored at -70°C until the virus could be quantitated. To do this, the lungs were thawed quickly in a 37°C waterbath then sonicated on ice to disrupt the lungs. The debris was sedimented at 3000 rpm for 10 min. After this, the supernatant was serially diluted and a plaque assay performed as previously described.

MDCK Cells: To determine the growth kinetics of the viruses *in vitro*, 35 mm culture dishes of confluent monolayers of MDCK cells were used. Infection of the MDCK monolayer follows the same protocol as for the radiolabelling of viral proteins except that the unadsorbed virus after 37°C incubation was washed off three times with warmed PBS before the overlay was added. This overlay was collected at time 0, 3, 6, 9, 12 and 24 hr, stored at -70°C until a plaque assay was performed by the standard method to quantitate virus.

Mouse Body Temperature

Mouse body temperatures were taken with a mouse rectal probe from Physitemp Instruments for 5 days preinfection in order to establish a baseline temperature for each mouse. Mouse infection was performed in triplicate as previously described for the two parental viruses and the two reassortants, J41 and W29. Temperatures were monitored until the more virulent viruses began to kill the mice.

Histopathology

Mice were inoculated with the viruses as described for the *in vivo* viral kinetics. On days 3 and 5 of infection the mice were sacrificed by 10% O_2 90% CO_2 asphyxiation in triplicate for each virus. The lungs and trachea were then exposed so that an 18 gauge needle attached to tubing containing 10% formalin in PBS under 25 cm head pressure could be inserted into the trachea to inflate the lungs with fixative. The lungs were left to fix for at least 30 min before being removed for storage in formalin. The lungs were then sectioned and stained with HPS at a pathology laboratory in the Civic Hospital, Ottawa to be ready for rating of pathology by Dr. B. Burns.

Fluorescent Immunostaining of Frozen Sections

Once again the mice were infected with influenza and sacrificed in the usual manner. Following exposure of the lungs and trachea, the lungs were inflated with a solution of Tissue-Tek OCT Compound (Fisher):PBS (1:1) using a syringe

and 18 gauge needle. Cross-sections were obtained from the center of the lung blocks. The lungs were then removed and immediately flash frozen in methylbutane resting in a bath of liquid nitrogen. The lungs were stored in methylbutane at -70°C until they could be sectioned in a cryostat. The cryostat was precooled to -20°C and the lungs were allowed to rise to this temperature before being cut into 8 μm thick sections. The dried sections were fixed on coverslips in anhydrous acetone at -20°C. Before immunostaining the OCT was removed by washing in PBS. The first reagent added to the coverslip for 30 min at room temperature was polyclonal rabbit serum to the virus at a 1:1000 dilution in PBS supplemented with 3% BSA and 0.01% sodium azide. After extensive washing in PBS the second reagent to be added also for 30 min at room temperature was a goat anti rabbit antibody labelled with fluorescein isothiocyanate (FITC) at a 1:160 dilution in the BSA supplemented PBS with 0.01% Evan's blue added as a counterstain. Fluorescent cells in approximately 150 to 200 fields per section were counted with sections from three different lungs per virus type.

Flow Cytometry

Mice were infected and sacrificed as before, but the lungs were inflated in this case with 1 ml of medium 199 containing 200 U of collagenase (Gibco). The lungs were then removed and minced in a further 4 ml of the medium with an additional 800 U of collagenase. This was incubated at 37°C for 2 hr

with rotary agitation. At the end of this time, the cells were forced through a 22 gauge needle using a syringe and allowed to incubate for another 30 min. The cells were then filtered through four layers of gauze, spun at 1000 rpm for 5 min, supernatant removed and the cells resuspended in 5 ml of ACK buffer to lyse the RBCs. After 5 min incubation at room temperature PBS was added to dilute the ACK buffer and the cells were spun again at 1000 rpm for 5 min. When the supernatant was removed the cells were resuspended in a minimum of 0.3 ml of normal mouse serum (Sigma) and incubated on ice for 1 hr. During this hour, the cells were counted using a hemocytometer so that approximately 2 x 10^6 cells could be used for each staining condition. The serum was removed from each aliquot by a 5 min 1000 rpm spin and the first antibody added was a lung adsorbed polyclonal rabbit anti-A/FM/1/47 at a 1:500 dilution in 40 μl of the same BSA/sodium azide containing PBS as in the frozen section staining. After a 30 min incubation on ice, this antibody was washed off with 10 ml of PBS containing 0.5% BSA and 0.05% sodium azide then spun at 1000 rpm for 5 min. The second antibody was a goat anti rabbit conjugated with FITC or phycoerythrin (PE) diluted 1:160 or 1:40 respectively in the 3% BSA containing buffer as for the first antibody. This was also incubated on ice for 30 min and then washed and spun in the manner described for the first antibody. At this point, the cells were ready for double staining for immune

cells with anti CD45 (B cells, Cedarlane), anti CD3 (T cells, Serotec) or anti Mac-1 (macrophages and neutrophils, Serotec) all labelled with FITC. These antibodies were diluted 1:16 once again in 3% BSA in PBS. The same 30 min incubation and washing steps were carried out as previously. The cells were then stained with 0.05 mg/ml propidium iodide (PI) for 1 min then washed again to detect dead cells. The cells were then ready for analysis in the flow cytometer (Coulter Epics XL-MCL. Apart from the polyclonal viral staining, a biotinylated monoclonal anti HA diluted 1:100 was also used with a secondary labelling with a 1:40 dilution of streptavidin conjugated to FITC. The cytometer was set up to detect the three flurochromes used in this protocol with sufficient colour compensation set ahead of time using single and double stained cells. Standardbrite beads (Coulter) were used before running of samples to ensure that the cytometer detection of fluorescence remained constant. The samples were syringed with a 25 gauge needle immediately before loading into the cytometer to protect the machine from clogging. Infection with each virus was repeated in triplicate for polyclonal antibody viral detection, viral and Mac-1, viral and CD45, viral and CD3, and anti HA monoclonal antibody along with appropriate prebleed serum and autofluorescent control for each of day 2, 3 and 5 postinfection.

Statistical Analysis

Replicate data were presented as mean value plus or minus 1 standard deviation, representing a 95% confidence interval. Standard deviation was calculated by the following formula:

$$s^2 = \frac{\sum_{i=1}^{n} (x_i - \bar{x})^2}{n - 1}$$

RESULTS

Sequencing

In order to determine the role of specific genes in the control of virulence it was first important to discover the genomic changes so that individual mutations could be related to the various virulence determinants.

Earlier genetic analysis has identified 4 genes that are associated with the increased virulence of FM-MA. Using Wilcoxin ranked sum analysis of FM-MA x HK reassortants, segments 4, 5, 7 and 8 were associated with virulence at the 0.1%, 5%, 1% and 5% levels of significance respectively (Brown, 1990). The purpose of this investigation was to compare the sequences of these genes of FM and FM-MA to identify mutations that control virulence.

Upon sequencing the cDNA clones of segments 4, 5, 7 and 8 of FM and FM-MA to find differences between them, only two changes were found in segment 4, one for segment 5, three for segment 7 and none for segment 8. Since there were no changes found for segment 8, new clones were chosen for FM and FM-MA segment 8 and sequenced. No chhanges were found in these new clones, so segment 8 could not be contributing to the virulence of FM-MA.

Having found changes in the cDNA of segments 4, 5 and 7, these sites were then checked by direct genomic RNA sequencing. Of the six changes that were checked by RNA sequencing, only three were actual mutations in the virus and

the other three were artifacts of cloning (see Table 2). The production of artifacts probably occurred during reverse transcription since the enzyme lacks a proof reading function. The mutations detected on RNA sequencing can be seen in Figure 2.

Segment 4 has a mutation at amino acid 47 of HA2 from a tryptophan (TGG) in FM to a glycine (GGG) in FM-MA. Segment 7 has two mutations, one silent mutation at a phenylalanine (TTT-TTC amino acid 32) and another at amino acid 139 from a threonine (ACC) in FM to an alanine (GCC) in FM-MA. The change seen on segment 5 cDNA was not present on genomic RNA. A summary of mutations found is shown in Figure 3, as a schematic representation of the 4 genome segments sequenced on FM and FM-MA. Also in Figure 3 is a depiction of some functional areas of the HA and M1 proteins that have been compiled by Carr and Kim in 1993, and Herlocher et al in 1992 respectively, which become important in an analysis of the possible role(s) that the mutations play in these properties of the proteins. The segment 4 mutation falls near the fusion peptide, and the segment 7 mutation is in the middle of a transcription inhibition region.

NCS Proteolysis

Knowing that mutation sites are present on only two of the four genes implicated in virulence allows the focus of this work to be narrowed. The first topic that will be presented is the characterization of the mutated hemagglutinin protein.

Table 2: Summary of Mutations in FM and FM-MA Segments 4, 5, 7 and 8 Determined by cDNA and vRNA Sequencing

Segment	Position	cDNA FM	cDNA MA	vRNA FM	vRNA MA	Occurrence of Mutation
4 (HA)	nt 560	CCG	CCA	CCA	CCA	cDNA cloning
	aa 162(HA1)	Pro	Pro	Pro	Pro	
	nt 1204	**TTG**	**GGG**	**TTG**	**GGG**	**vRNA**
	aa 47(HA2)	**Trp**	**Gly**	**Trp**	**Gly**	
5 (NP)	nt 1496	GAA	GGA	GAA	GAA	cDNA cloning
	aa 482	Glu	Gly	Glu	Glu	
7 (M1, 2)	**nt 121**	**TTT**	**TTC**	**TTT**	**TTC**	**vRNA**
	aa 32(M1)	**Phe**	**Phe**	**Phe**	**Phe**	
	nt 360	GAC	GCC	GCC	GCC	cDNA cloning
	aa 112(M1)	Asp	Ala	Ala	Ala	
	nt 440	**ACC**	**GCC**	**ACC**	**GCC**	**vRNA**
	aa 139(M1)	**Thr**	**Ala**	**Thr**	**Ala**	
8 (NS1, 2)						no mutations

Figure 2: Viral RNA Sequence of Mutation Sites

An RNA sequence gel to confirm the presence of mutation in segment 4 (HA2-47) and segment 7 (M1-32 and M1-139) of FM compared to FM-MA. The sequence is listed in the margin, and the small open arrow on the photograph indicates the position of the mutation site. The nucleotide order for the four sequencing lanes is A, C, G, T.


HA2-47
FM I MA
M1-32
FM I MA
M1-139
FM I MA

Figure 3: Map of Mutations on Segments 4, 5, 7 and 8

A summary of the mutations found on the four segments of FM and FM-MA that were sequenced. No mutations were detected for segments 5 (NP) and 8 (NS1, 2). Amino acid changes are indicated at the mutation sites. The location of the proteolytic cleavage site that produces the HA1 and HA2 subunits of HA is identified with an arrow. The fusion peptide of HA (HA2 a.a. 1-25) is also indicated by a gray box. A functional map of M1, compiled by Herlocher et al, shows the lipid binding regions labelled with checked boxes, RNA and RNP binding regions with black boxes and the zinc finger motif location with an open box.

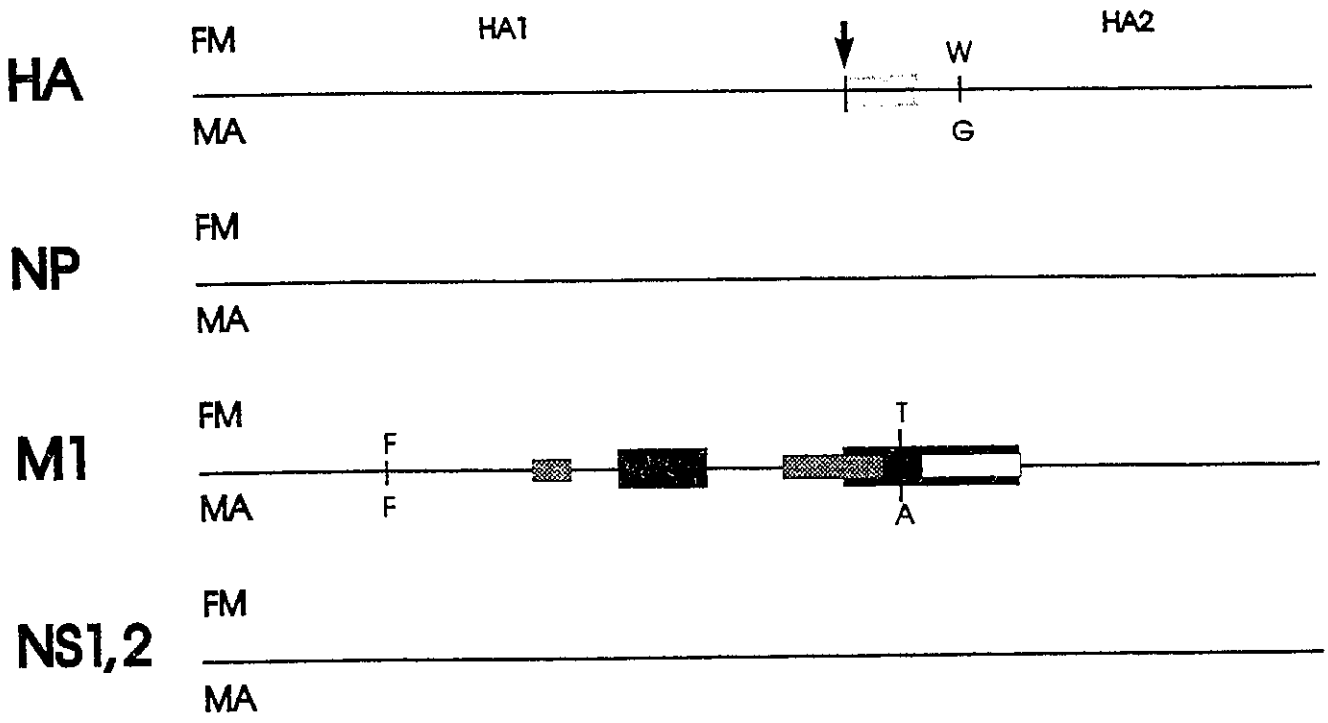
HA
FM
HA1
HA2
W
MA
G
NP
FM
MA
M1
FM
T
F
F
MA
A
NS1,2
FM
MA

This is dealt with in two parts, with a structural analysis using chemical cleavage of the tryptophan residues followed by a functional assay of the HA protein fusion property. Since the mutation was from a tryptophan in FM to glycine in FM-MA, N-chlorosuccinimide was used to partially cleave the proteins at the tryptophans by oxidative chlorination of the tryptophanyl peptide bonds (Shechter et al, 1976). With FM having an extra tryptophan compared to FM-MA, it would be expected that FM would have unique cleavage products as a result. Analysis of cleavage products by SDS-PAGE should produce a different banding pattern for the HA proteins of the two viruses. To reduce the complexity of the banding pattern produced, only HA2 was used for NCS cleavage. The first step in this process was the immune precipitation of labelled HA from infected MDCK cells followed by trypsin cleavage of HA0 to yield HA1 and HA2. Figure 4 is an autoradiograph of the labelled viral proteins (lanes 2 and 4), the supernatant after immune precipitation (lanes 1 and 3) and the precipitated HA of FM and FM-MA after cleavage with two concentrations of trypsin (lanes 5 - 8). It is apparent, especially with the more concentrated trypsin (lanes 7 and 8), that the trypsin cleavage products of FM HA differ from FM-MA HA. FM HA is nearly entirely cleaved into HA1 and another product smaller than HA2 along with a reduced amount of HA2. A very small portion of the HA of FM-MA is also cleaved into this smaller peptide but the majority of

Figure 4: Immune Precipitation and Trypsin Cleavage of HA Protein

The ^{35}S-methionine labelled influenza proteins from an infected cell lysate were run on a 12.5% SDS-PAGE. Lanes 1 and 3 show the influenza proteins remaining in the supernatant of FM and FM-MA infected cell lysates after immune precipitation with an anti-HA monoclonal antibody (H9D3-4R2). Lanes 2 and 4 show the cell lysate before immune precipitation for FM and FM-MA respectively. Lanes 5 and 6 were loaded with the precipitated HA cleaved with 0.5 μg/ml trypsin of FM and FM-MA respectively. The HA in lanes 7 and 8 was treated with 1 μg/ml trypsin once again from FM and FM-MA.

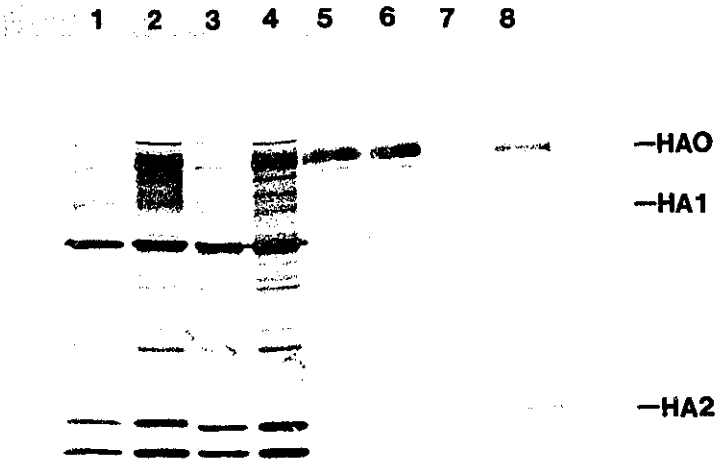
1
2
3
4
5
6
7
8
—HAO
—HA1
—HA2

the cleavage results in HA1 and HA2. This indicates that in addition to the normal cleavage site between HA1 and HA2 there is another trypsin cleavage site in HA2 that is more susceptible in the case of FM virus.

Having produced the required HA2 by preparative SDS-PAGE, the NCS cleavage could be carried out. In Figure 5, comparing lanes 1 and 2 or lanes 3 and 4, there is, as expected an obvious difference in banding patterns between FM and FM-MA due to the difference in tryptophans. There is also an unanticipated shift in the uncleaved portion of the HA2 (221 a.a.), further complicating the already difficult task of assigning sizes to the peptides from predicted values. The size of peptide fragments was estimated by the Coomassie blue stained markers and the expected sizes of fragments predicted by the location of tryptophan residues. In partial proteolysis mapping, the most abundant cleavage products usually result from single rather than double cleavage (Brown, 1981). The largest peptide fragment of approximately 174 amino acids is only seen below the uncleaved FM HA2 band of 221 amino acids. This peptide results from cleavage at tryptophan of HA2 amino acid 47 that is not present in FM-MA HA2. The difference in trypsin sensitivity, electrophoretic mobility of HA2 and NCS cleavage pattern all indicate a mutation in HA2 at the tryptophan.

Throughout the rest of the results section it is useful to

Figure 5: N-chlorosuccinimide Cleavage of Tryptophans in HA2

This is an autoradiograph of a 17.5% SDS-PAGE loaded with NCS cleaved ^{35}S-methionine labelled HA2 proteins. The marker proteins shown in the left margin were: lactoglobulin, 162 a.a. (MW 18 360); sperm whale myoglobin, 153 a.a. (MW 17 816) and horse cytochrome c, 105 a.a. (MW 12 384). Lanes 1 and 2 contain HA2 cleaved with 1.5 mM NCS from FM and FM-MA respectively. In lanes 3 and 4, FM and FM-MA proteins were cleaved with 15 mM NCS. The estimated amino acid lengths of the fragments are listed in the right margin. These are taken from the map of tryptophans numbered on HA2 with the mutated tryptophan in brackets, as shown below. The radioactive methionine incorporation sites are marked with an asterisk.

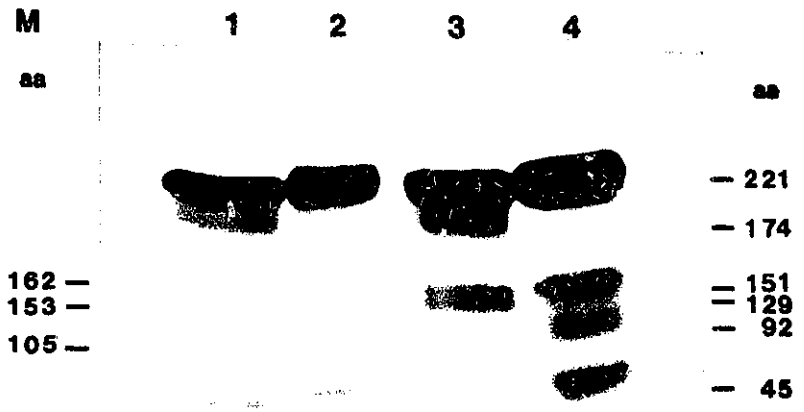
M
1
2
3
4
aa
aa
162
153
105
221
174
151
129
92
45

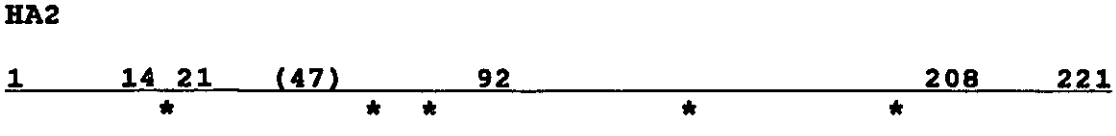
HA2
1
14
21
(47)
92
208
221

keep in mind that all of the viral reassortants whose name begins with a J, are composed of segment 4 from FM-MA on an FM background and the W and T series of reassortants have segments 4 and 7 or 4, 7 and 8 of FM-MA on an FM background respectively. Since segment 8 of FM and FM-MA are unchanged, W and T reassortants are expected to be identical.

Hemolysis

Amantadine resistant mutants have been seen to include mutations at amino acid 47 of HA2 from glutamine to arginine and glutamine to leucine (Wiley and Skehel, 1987). These amantadine resistant mutants also demonstrated a change in their optimum pH of fusion. We were interested in knowing how the mutation from tryptophan to glycine at this position 47 of HA2 in FM and FM-MA affected the pH optimum of fusion. To characterize the optimal pH of fusion a hemolysis assay is normally carried out. In this study, both parental viruses and two reassortants containing segment 4 or segments 4 and 7 of FM-MA on a background of FM were tested to determine if the pH at which their hemagglutinin trimers undergo a conformational change to result in fusion and then lysis of the RBC to which they are attached is different. From Figure 6, the 50% of maximum hemoglobin release, which by convention is considered the optimum pH of fusion, can be calculated for each of the viruses tested (Doms et al, 1986). All of the viruses containing the HA of FM-MA (i.e. all viruses tested except for FM) have a pH optimum of 5.5 with

Figure 6: Hemolysis Assay for the Detection of Fusion Mutants

The extent of hemoglobin release from damaged RBCs due to HA conformational changes for fusion at low pH is shown on the vertical axis. This is expressed as a percentage of the maximum release detected in supernatants by spectrophotometer. Four viruses were tested in triplicate including: FM - open circle, J41 - open triangle, W29 - open diamond and FM-MA - open square. Error bars indicate ±1 standard deviation.

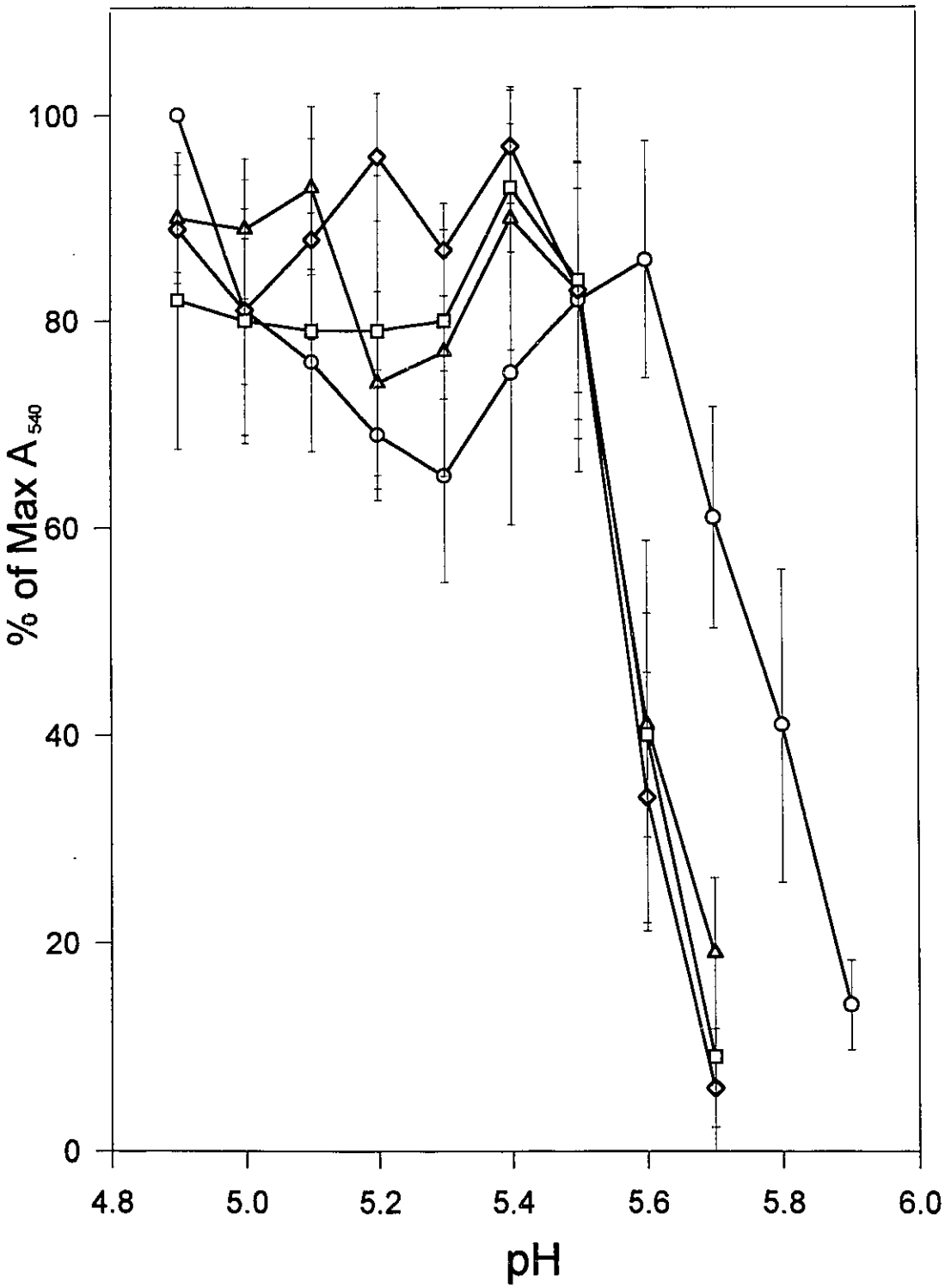
100
80
60
40
20
0
% of Max A540
4.8
5.0
5.2
5.4
5.6
5.8
6.0
pH

FM alone having an optimum 0.2 pH units higher at 5.7. All of the viruses sharing the FM-MA HA have nearly identical profiles of fusion response with respect to pH.

Previous genetic analysis indicated that segments 4 and 7 were responsible for most of the acquired virulence of FM-MA since reintroduction of these genes into FM virus produces viruses that are almost as virulent as FM-MA. Sequencing, chemical proteolysis and an *in vitro* functional assay have established that there are changes in the hemagglutinin of FM-MA compared with FM, and similarly for the M1 gene, sequencing and the observation of protein shift in SDS-PAGE (see Appendix 3) indicates that there are changes in the matrix protein as well. The rest of the results section will be concerned with the tests for biological importance of these changes.

Viral Growth Kinetics in Mouse Lung

The growth success of viruses is measured by rate and extent of production of infectious units of virus.

In the first set of viral growth experiments, the viruses were grown in mouse lung. The viruses used were the parental strains FM and FM-MA, and all of the reassortants derived from them: J41 that has segment 4 from FM-MA, W29 that has segments 4 and 7 from FM-MA and TSR17 that has segments 4, 7 and 8 from FM-MA.

In Figure 7 the growth in mouse lung of the two parental viruses is plotted. It is apparent, especially at early time

Figure 7: Growth Kinetics of Virus in Mouse Lung

Each point is the geometric mean titer of three pools of three lungs with error bars of ± 1 standard deviation. The two parental viruses are shown.
FM - open circle
FM-MA - open square

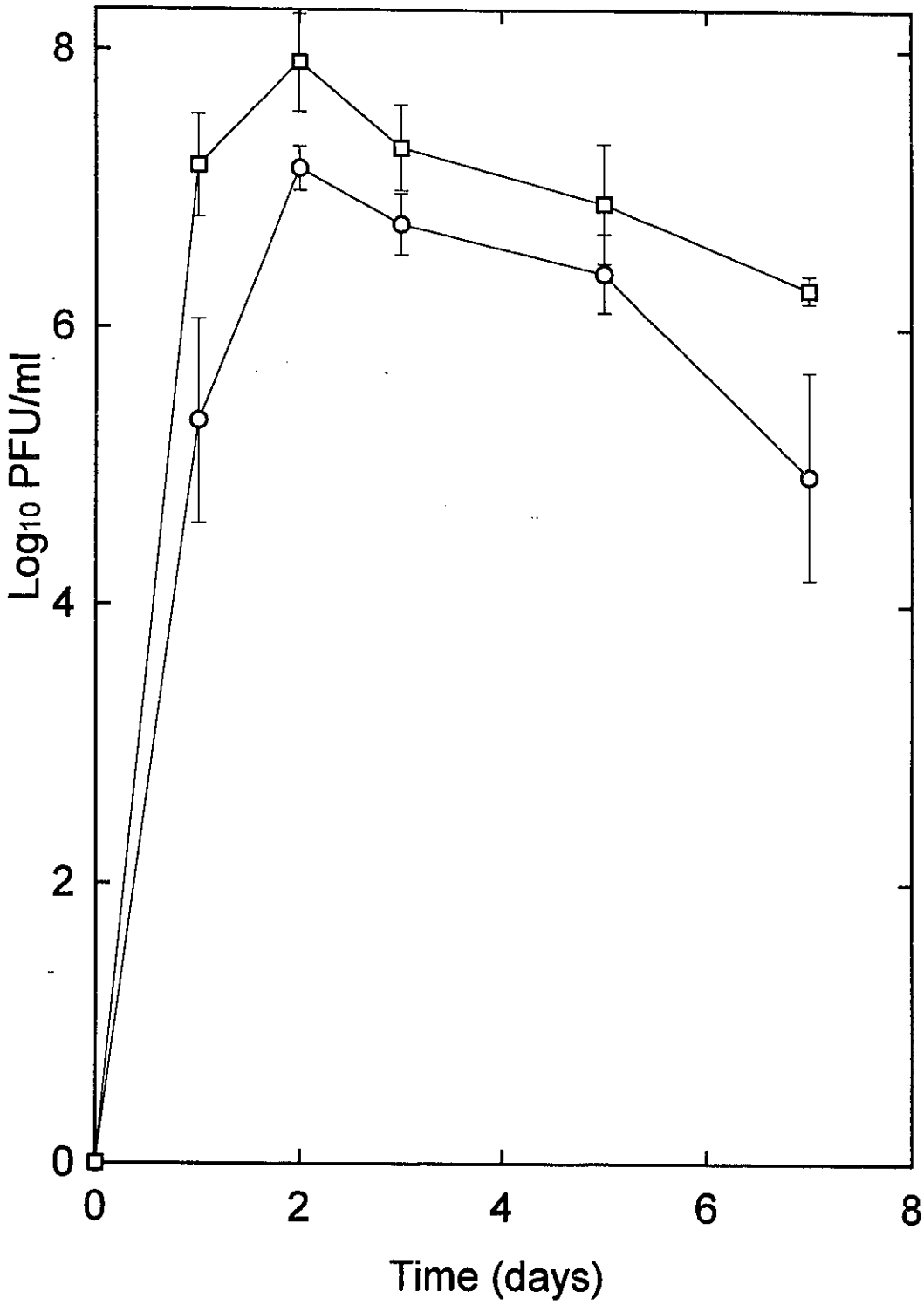
8
6
4
2
0
Log10 PFU/ml
0
2
4
6
8
Time (days)

points, that FM-MA grows both faster than FM and to a higher titer. FM-MA actually grows to nearly 1 log higher titer in mouse lung than FM. Since variability is observed in these experiments due to animal variability and the nature of plaque assays, the experiments are done in triplicate, each experiment using 3 mice for each timepoint and virus. Other factors in this variability are the critical timing of the lung harvest, especially early in the experiment as well as the fact that by day 6 or 7 some of the mice infected with the more virulent viruses are dying so those remaining alive may not be entirely representative.

Figure 8 demonstrates the effect of adding segment 4 of FM-MA to an FM background. Apart from a slight suggestion on day 1 that J41 might grow faster than FM, there appears to be no growth advantage imparted by segment 4. Figure 9 however, shows the importance of segments 4 and 7 or 4, 7 and 8 with viruses W29 and TSR17 respectively. The growth of these two viruses closely follows that of FM-MA so it appears that segment 7 allows for faster growth of virus whereupon it reaches higher titers comparable to FM-MA. Maximum titers for all viruses are observed on day two.

Figure 10 serves to give a more detailed picture of the early events in infection with closer time intervals than in Figures 7 to 9. Here with time intervals of every 6 hours, it is still apparent that viral titers climb steadily to a maximum at day 2. It is also apparent from this figure that

Figure 8: Growth Kinetics of Virus in Mouse Lung - Role of Segment 4

Each point is the geometric mean titer of three pools of three lungs with error bars of ± 1 standard deviation. The two parental and segment 4 reassortant viruses are shown.
FM - open circle
FM-MA - open square
J41 - open triangle

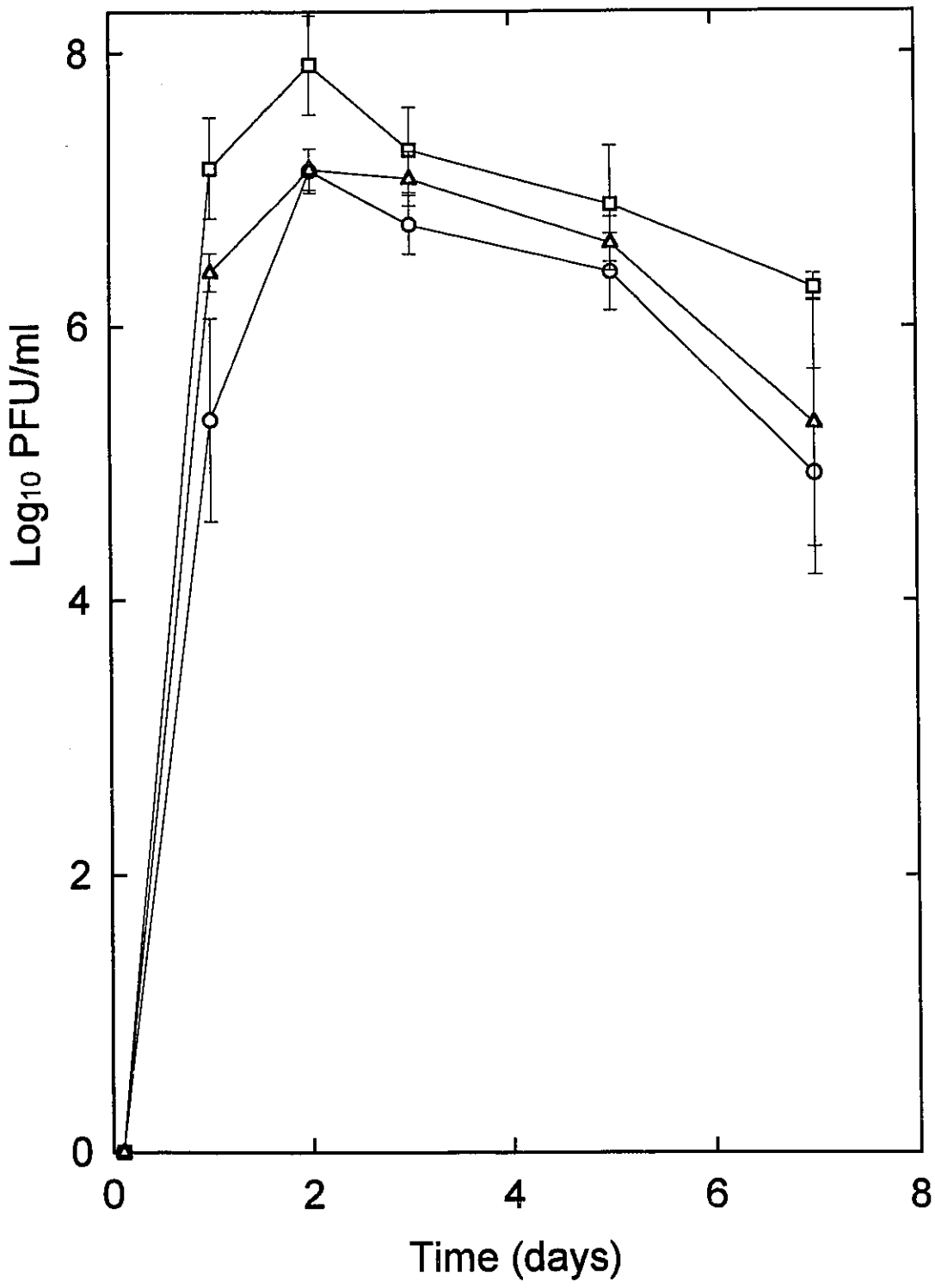
8
6
4
2
0
Log10 PFU/ml
0
2
4
6
8
Time (days)

Figure 9: Growth Kinetics of Virus in Mouse Lung - Role of Segments 4 and 7

Each point is the geometric mean titer of three pools of three lungs with error bars of ± 1 standard deviation. The two parental, the segment 4 and 7 and the segment 4, 7 and 8 reassortant viruses are shown.
FM - open circle
FM-MA - open square
W29 - open diamond
TSR17 - closed inverted triangle

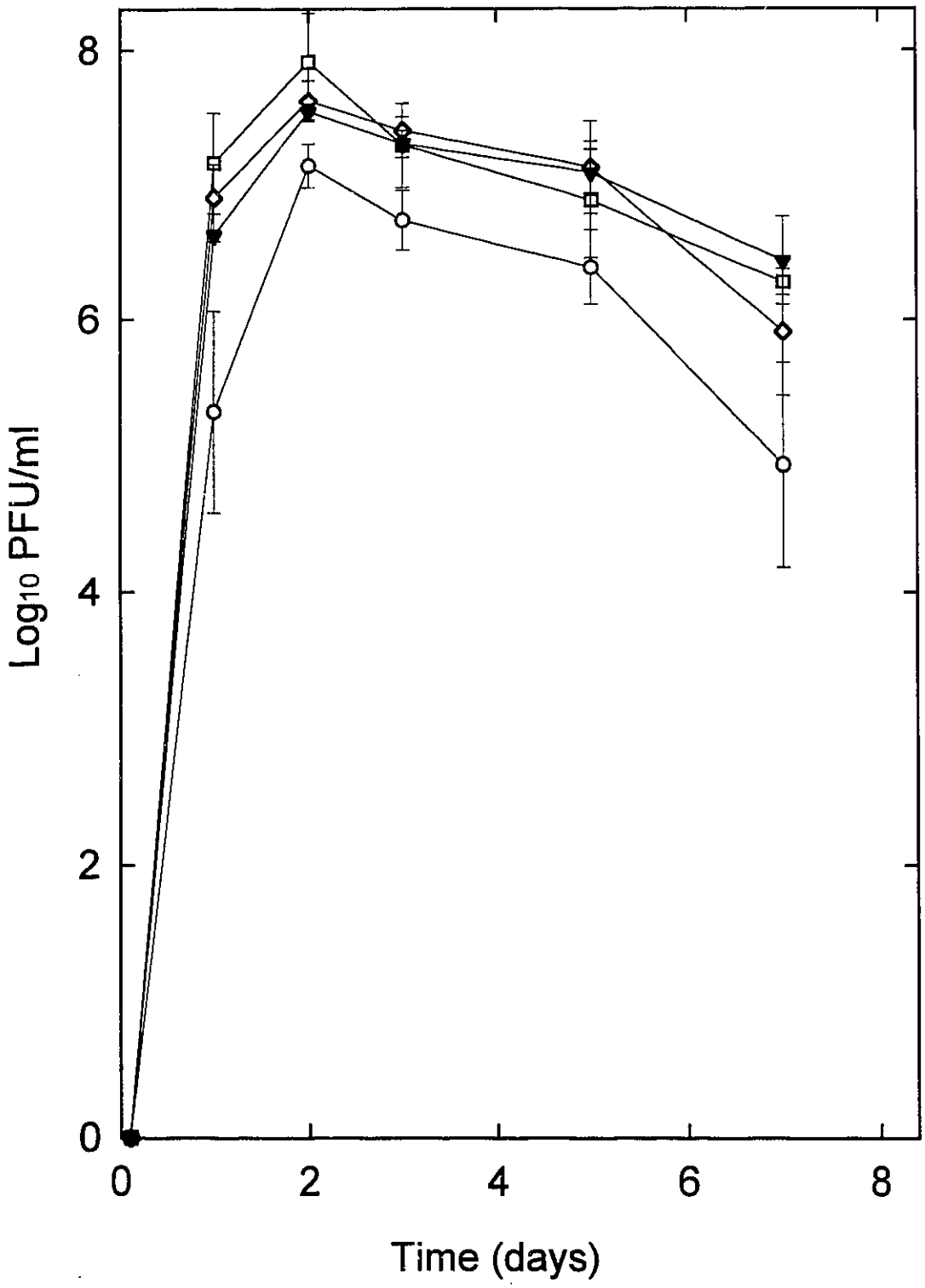
8
6
4
2
0
Log10 PFU/ml
0
2
4
6
8
Time (days)

Figure 10: Growth Kinetics of Virus in Mouse Lung - Early Timepoints

Each point is the titer of a pool of three lungs. Samples were taken every six hours to establish the relationship of the segnment 4 reassortant to the parentals.
FM - open circle
FM-MA - open square
J41 - open triangle

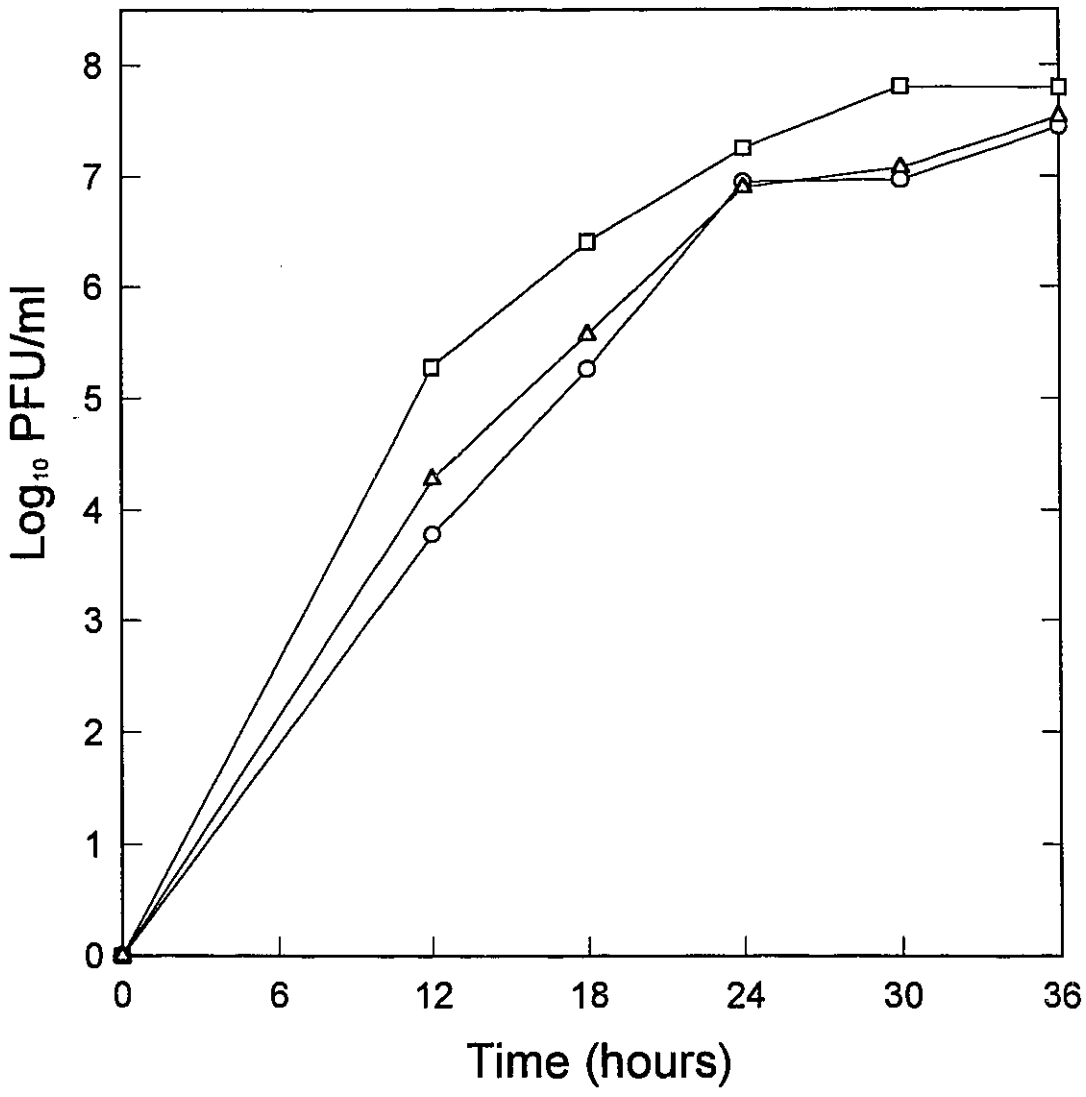
Log10 PFU/ml
0
1
2
3
4
5
6
7
8
0
6
12
18
24
30
36
Time (hours)

the advantage that J41 appeared to have on day 1 of infection in Figure 8 is not borne out by this graph. Both J41 and the FM parent follow the same growth curve.

Viral Growth Kinetics in MDCK Cell Culture

The same growth kinetics experiments as in the mouse lung are repeated here with the addition of two new reassortant viruses; J9 having segment 4 of FM-MA and T154 having segments 4, 7 and 8 of FM-MA. The timing for these *in vitro* experiments is also different due to the fact that in 24 hours the cell monolayers demonstrate a cytopathic effect (CPE) and virus titers are starting to drop by this time. The same pattern of results are seen *in vitro* as in the *in vivo* mouse lung experiment. Figure 11 again shows the parental viruses alone. FM-MA grows both faster and to a higher final titer than FM with this titer difference being most apparent at later times during the study. Figure 12 shows the contribution that segment 4 of FM-MA makes on the growth of virus *in vitro*. On this graph, the two J viruses flank FM, demonstrating that they are capable only of the same growth as the non-adapted parent. When segment 7 is added to segment 4 as in Figure 13, once again these reassortant viruses have the same growth advantage as MA. All of the viruses have their peak titer a 9 hours post infection, with the exception of J41 that has its peak 3 hours later.

In conjunction with detecting the amount and speed of

Figure 11: Growth Kinetics of Virus in MDCK Cells

Each point is the geometric mean titer of three replicate experiments with error bars of ± 1 standard deviation. The two parental viruses are shown.
FM - open circle
FM-MA - open square

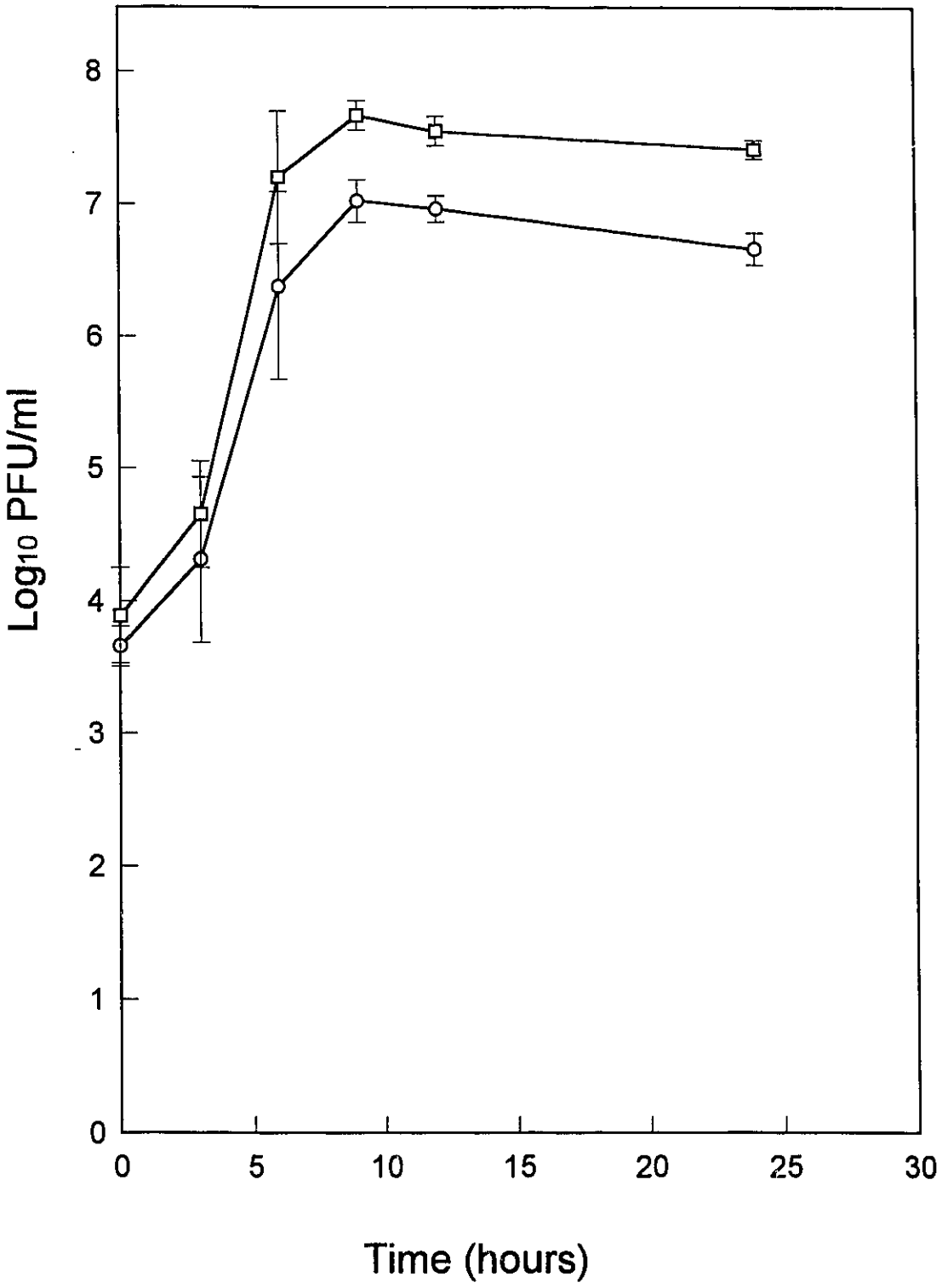
Log10 PFU/ml
0
1
2
3
4
5
6
7
8
0
5
10
15
20
25
30
Time (hours)

Figure 12: Growth Kinetics of Virus in MDCK Cells - Role of Segment 4

Each point is the geometric mean titer of three replicate experiments with error bars of ± 1 standard deviation. The two parental and the segment 4 reassortant viruses are shown.
FM - open circle
FM-MA - open square
J41 - open triangle
J9 - open inverted triangle

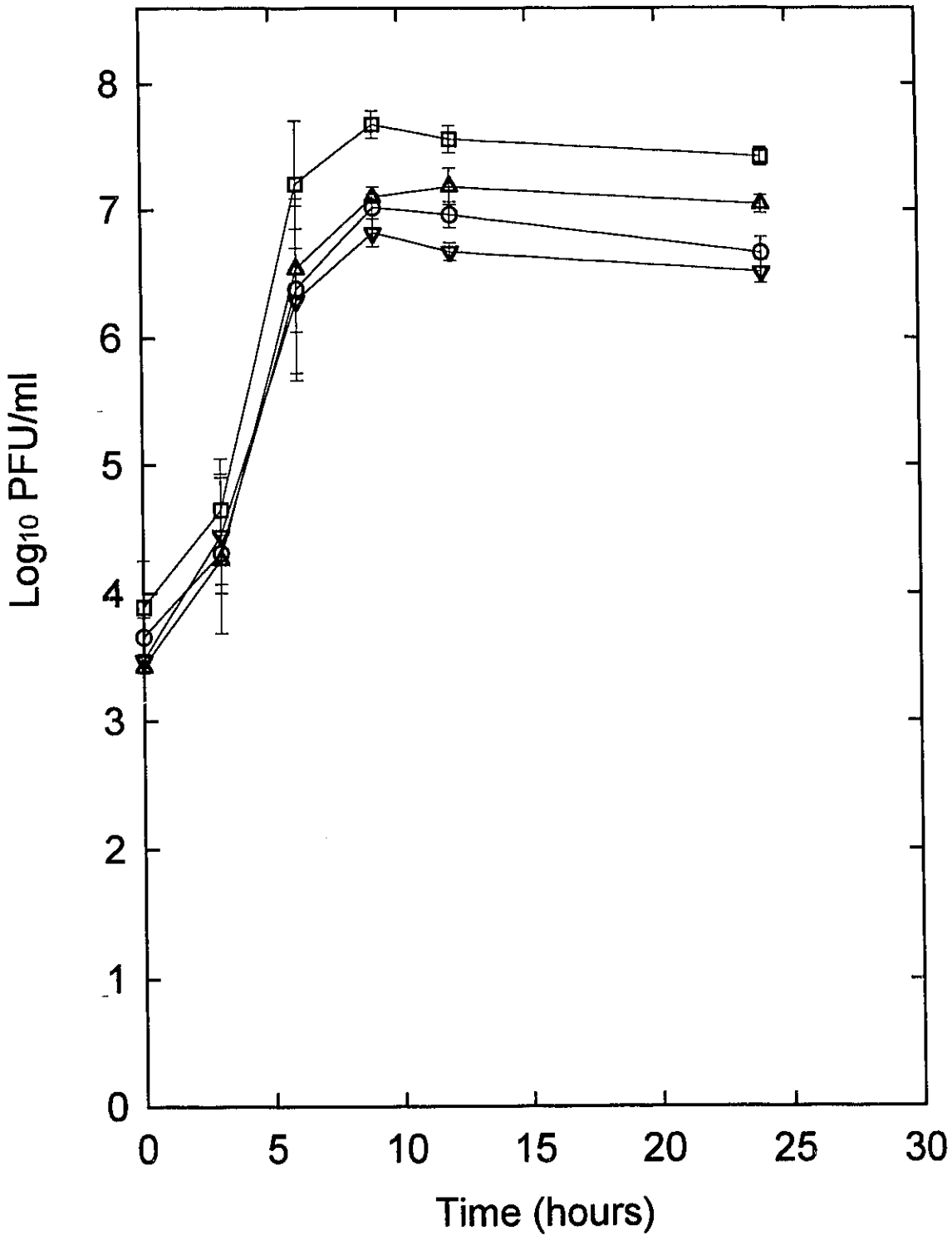
Log10 PFU/ml
0
1
2
3
4
5
6
7
8
0
5
10
15
20
25
30
Time (hours)

Figure 13: Growth Kinetics of Virus in MDCK Cells - Role of Segments 4 and 7

Each point is the geometric mean titer of three replicate experiments with error bars of ± 1 standard deviation. The two parental, the segment 4 and 7 and 4, 7 and 8 reassortant viruses are shown.
FM - open circle
FM-MA - open square
W29 - open diamond
T154 - closed triangle
TSR17 - closed inverted triangle

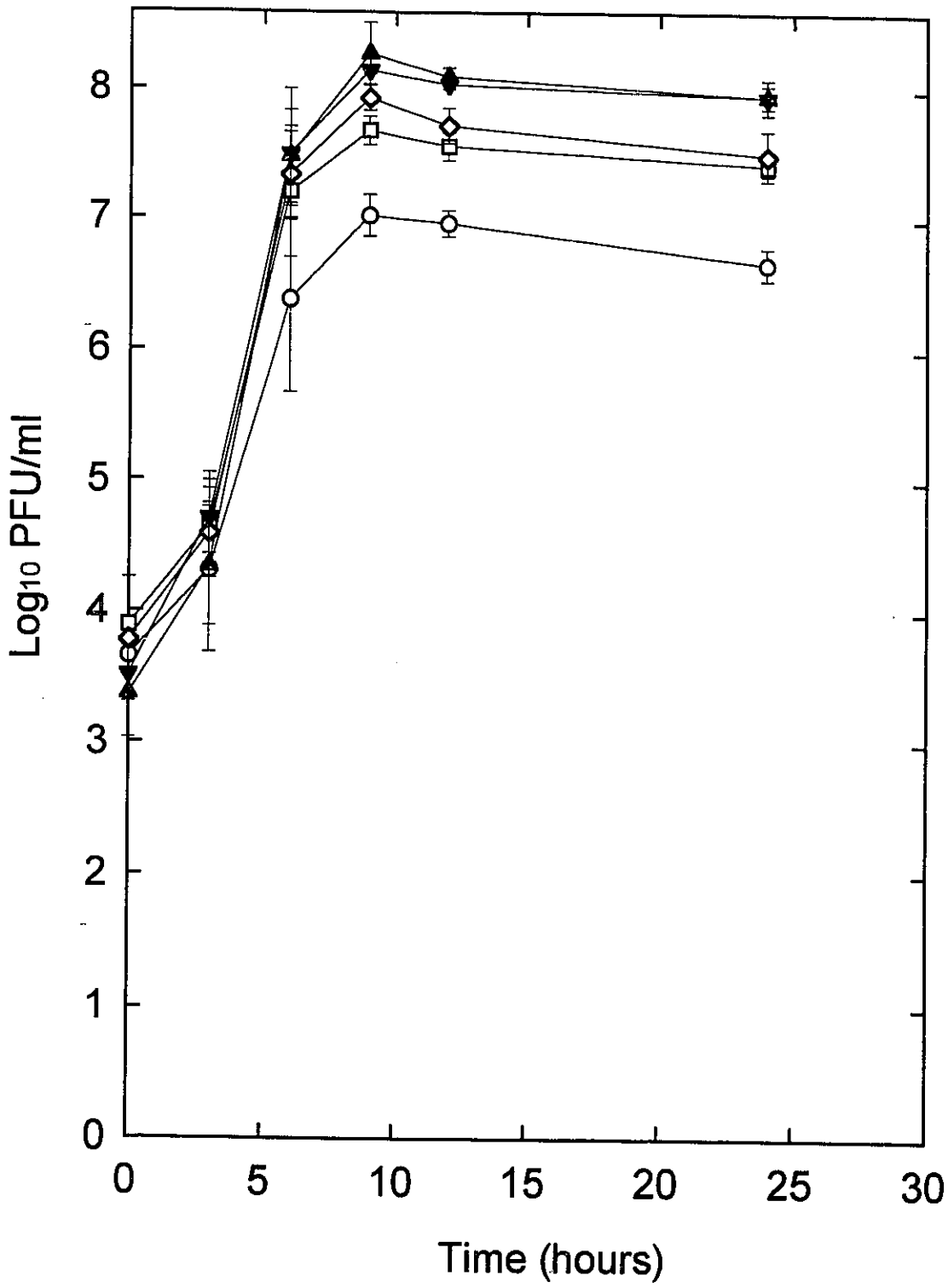
Log10 PFU/ml
0
1
2
3
4
5
6
7
8
0
5
10
15
20
25
30
Time (hours)

viral growth in the lungs of mice and cell monolayers, a study of the effect that this growth is having on the lung tissue of the mouse was also made in order to explain more fully the virulence differences demonstrated by the viruses. This included standard histopathology, a measurement of body temperature, location of infected cells with immunologically stained frozen section and a flow cytometer count of infected cells with a concomitant count of immune cells.

Mouse Temperatures

Monitoring the temperature of mice while infected with influenza was a very convincing method for measuring the deterioration of lethally infected animals. In Figure 14, groups of 3 mice were monitored while infected with FM, FM-MA, J41, and W29 viruses and compared to mock infected mice. For the first 5 measurements, the baseline temperature for each mouse was established, which on average was between 36°C and 37°C. It appears that there may be only a slight drop in temperature soon after infection (or mock infection) in the control, FM and J41 mice that is restored by day 7. The two more virulent viruses, W29 and FM-MA show a much different trend. Immediately after infection, their temperatures begin to drop similar to the others, but instead of recovering by day 7 their temperatures begin to drop precipitously beginning on day 5 until their body temperature reaches approximately 33°C whereupon they begin to die. Body temperatures as low as 28.8°C were recorded 10 days post-

Figure 14: Mouse Rectal Temperatures

Mouse temperatures were taken for five days prior to the intranasal installation of virus to establish a baseline temperature for each mouse. Points on the figure represent the average of the deviations of each mouse's temperature from their average baseline temperatures in the three mice tested per virus strain. Control mice were mock infected using PBS.

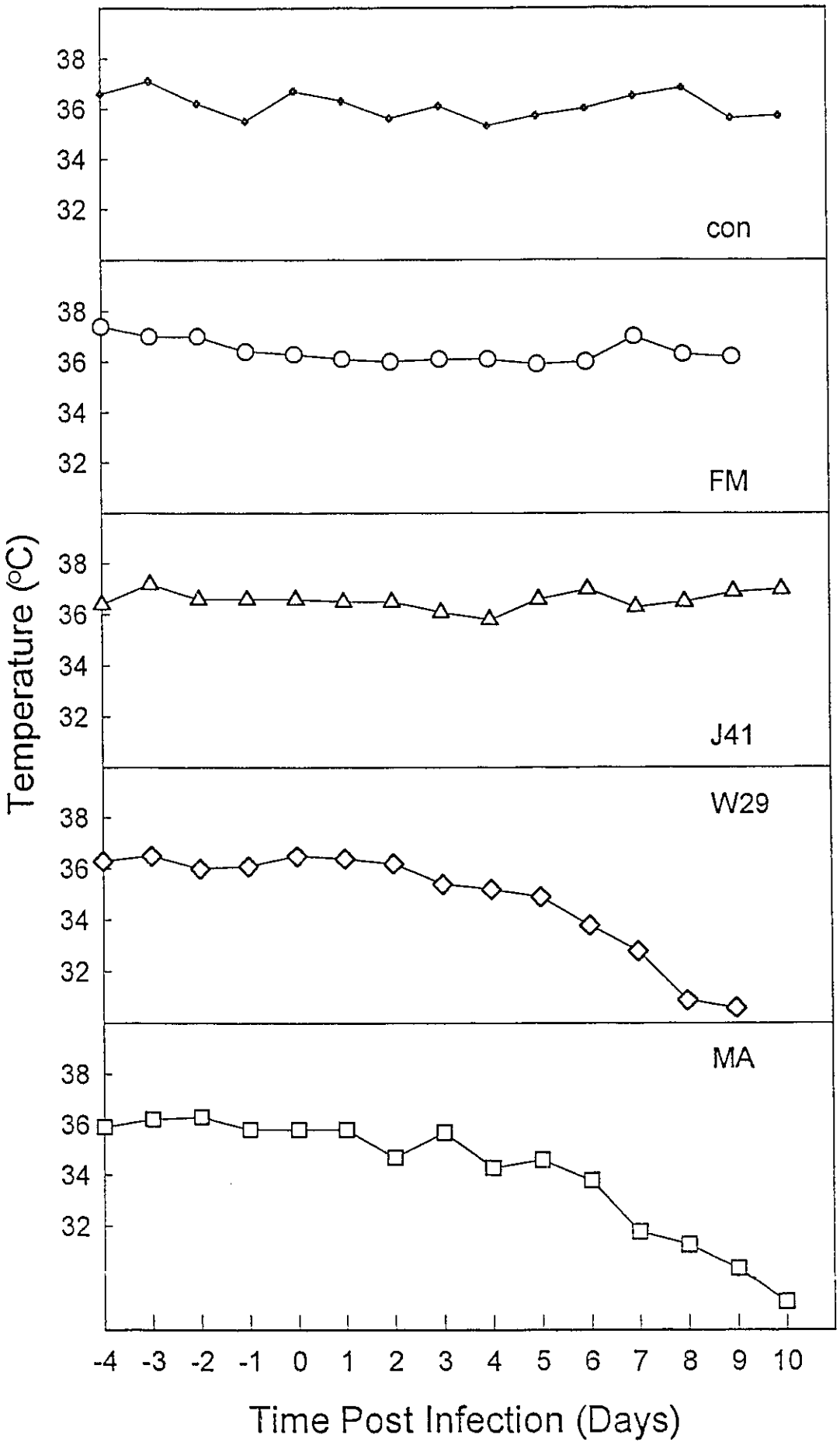
Temperature (°C)
38
36
34
32
con
FM
J41
W29
MA
-4 -3 -2 -1 0 1 2 3 4 5 6 7 8 9 10
Time Post Infection (Days)

infection for mice infected with FM-MA and W29 viruses.The remaining mice were euthanized at this time because of their deteriorating condition.

Pathology - HPS Sections

In order to see the damage and immune cell infiltration in the mouse lungs due to viral infection, formalin fixed sections of infected lungs were stained and numerically rated for the extent of pathology. Figure 15 is a composite of these sections taken on days 3 and 5 post infection and it demonstrates that different viruses induce different amounts of pathology. In the control lung, the epithelium lining the bronchioles retains its slightly ridged, but continuous layer of epithelial cells, while in all of the virus infected lungs the airway has been denuded and dead cells are sloughing off into the lumen of the airway. There are also many immune cells encircling the bronchioles with the extent of this increasing by day 5. As for the alveoli, in the control they show few immune cells and have clear airspaces, while the virus infected lungs show patches of infiltrating inflammatory cells, areas of hemorrhage and some evidence of interstitial thickening characteristic of viral pneumonia. Some of the most extensive damage can be seen for viruses W29 and MA both on days 3 and 5, although it should be noted that all of these photographs were taken in the most damaged, highly infiltrated areas that could be found on each section. It is evident that both FM and J41 demonstrate

Figure 15: Influenza Infected Mouse Lung Pathology

This composite is made up of photographs taken of formalin fixed HPS stained mouse lung sections that are showing signs of severe damage 3 and 5 days after viral infection. The photographs were taken in focal areas of destruction and are not representative of the entire lung sections.

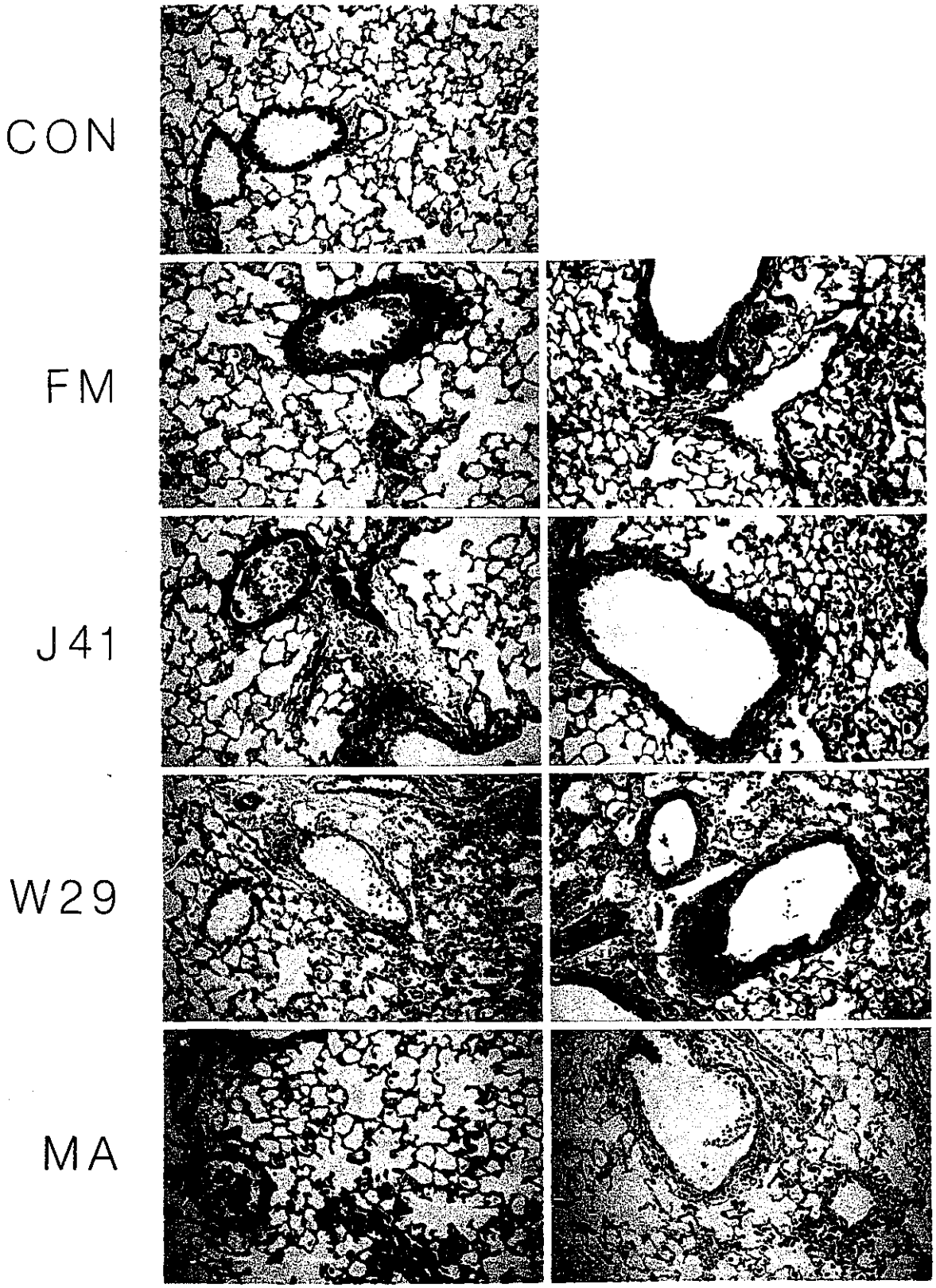
D3
D5
CON
FM
J41
W29
MA

considerable lung involvement in the pictures shown and that these foci of inflammation are much fewer in number than W29 and FM-MA. The following figure, Figure 16 gives a numerical representation to the inflammatory changes present as graded by pathologist Dr. B. Burns, Dept. of Pathology, University of Ottawa, in a blind assessment of pathology. Figures 16A and B show little differences between viruses in peribronchial lymphocyte infiltration or necrosis of bronchial epithelium. Polymorphonuclear leukocyte (PMN) infiltration typically occurs early in infections and is short lived, being replaced by other inflammatory cell types. In this investigation, there may be some evidence for this with regard to FM-MA whose rating has dropped by day 5. It is difficult to discern more from this graph because the error bars are overlapping. Peribronchial lymphocytes do not appear to change over the course of infection for all viruses tested. In the lower portion of the figure, the interstitial lymphocytes and bronchopneumonia ratings show some interesting differences. In bronchopneumonia, which is a measure of the lung consolidation in the airspaces with fluid, cells and debris, the rating for FM increases as well as that for W29 from day 3 to day 5. There is no detectable difference in J41 and FM-MA. With interstitial lymphocytes, the trend seems to be that FM and J41 show less evidence of this alveolar wall thickening than W29 and MA at both timepoints although the difference is greatest on day 3.

Figure 16: Pathology Ratings for Influenza Infected Mouse Lungs

The HPS stained lung sections were rated by pathologist Dr. B. Burns on a scale of 0 to 3 with a rating of 3 reserved for only the most severly affected lungs under four categories. These categories include: (A) peribronchial lymphocytes, (B) necrosis of bronchial epithilim - PMNs, (C) bronchopneumonia, and (D) interstitial lymphocytes. The histograms are the average of the ratings of three lungs with error bars of ± 1 standard deviation.
Control - open box
FM - diagonal up to the right
J41 - diagonal down to the right
W29 - crosshatched box
FM-MA - horizontal lines

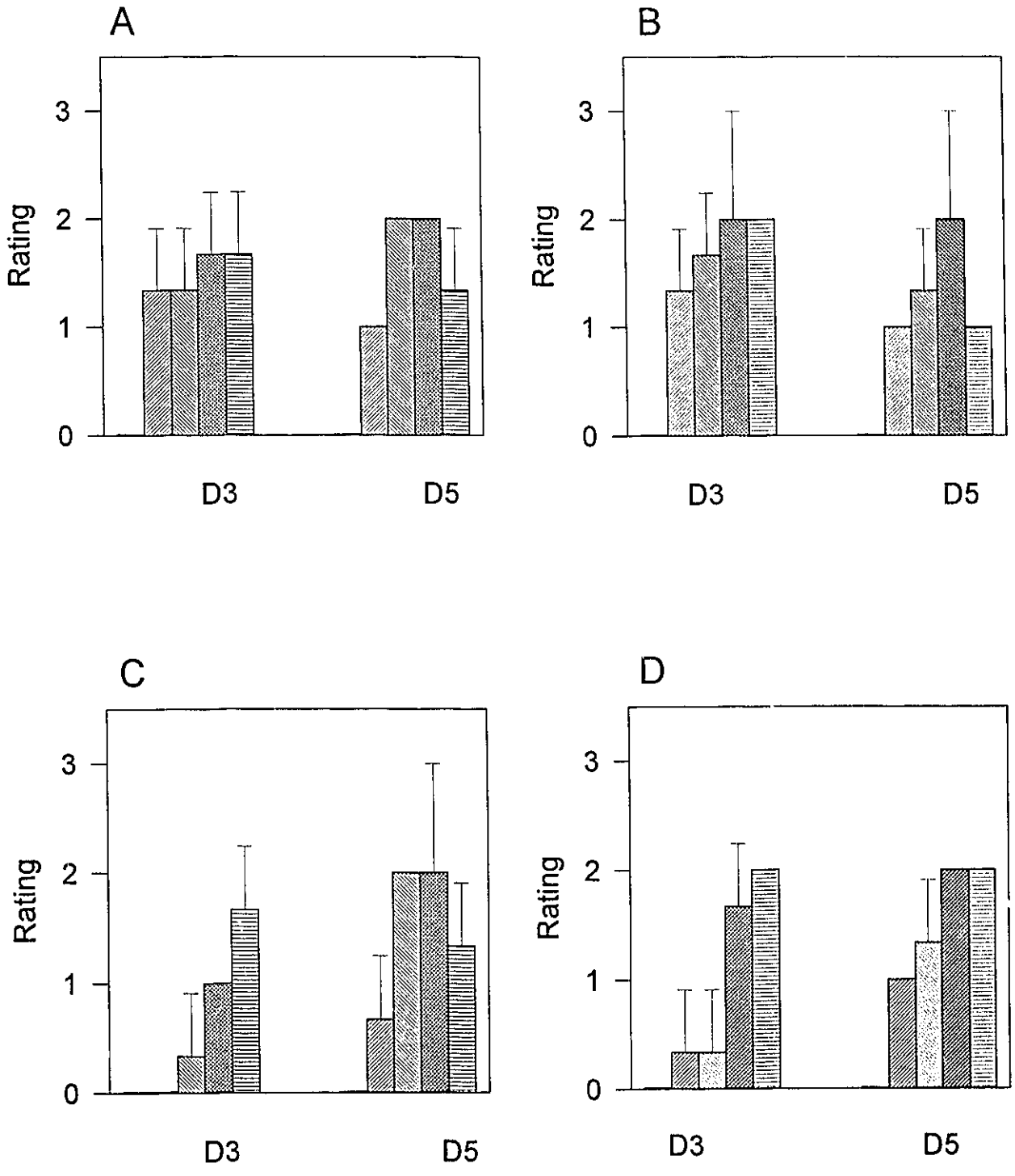
A
B
C
D
Rating
0
1
2
3
D3
D5

Pathology - Fluorescent Antibody Stained Sections

As it had been determined that viral titers are different for the parental viruses as well as the reassortant viruses in the mouse lung and the pathology report showed some differences in inflammatory response in the mouse lung as well, it seemed important to determine if more cells are actually infected by these viruses in the lung. It would also be informative to find out if perhaps different cell types are affected with the different viruses thus explaining some of the differences seen in virulence. To do this, acetone fixed frozen lung sections were stained with a rabbit polyclonal anti-influenza immune serum (αFM) followed by a secondary anti-rabbit IgG antibody labelled with FITC. Figure 17 is a composite of these viral antigen stained lung sections over three time periods for the two parental and two reassortant viruses. Once again, as in the HPS stained section composite, this composite is a collection of photographs of focal areas of infection in the lung section and this type of staining doesn't necessarily represent that of the entire lung. Throughout the timepoints, there is a progression of infection. For example, on day 2 of infection it is rare to see much alveolar involvement except in the MA infection. By day 5, the likelihood of finding fluorescent alveoli is much increased. Apart from FM, which does not seem to have stained as brightly positive as the other viruses have, there are no differences in staining between

Figure 17: Fluorescent Antibody Staining for Influenza Antigens in Infected Mouse Lung

This composite is made up of photographs of FITC conjugated antibodies labelling influenza antigens on frozen sections of mouse lung harvested 2, 3 and 5 days post-infection. The photographs were taken in the most brightly fluorescing areas, and may not be representative of the entire lung section.

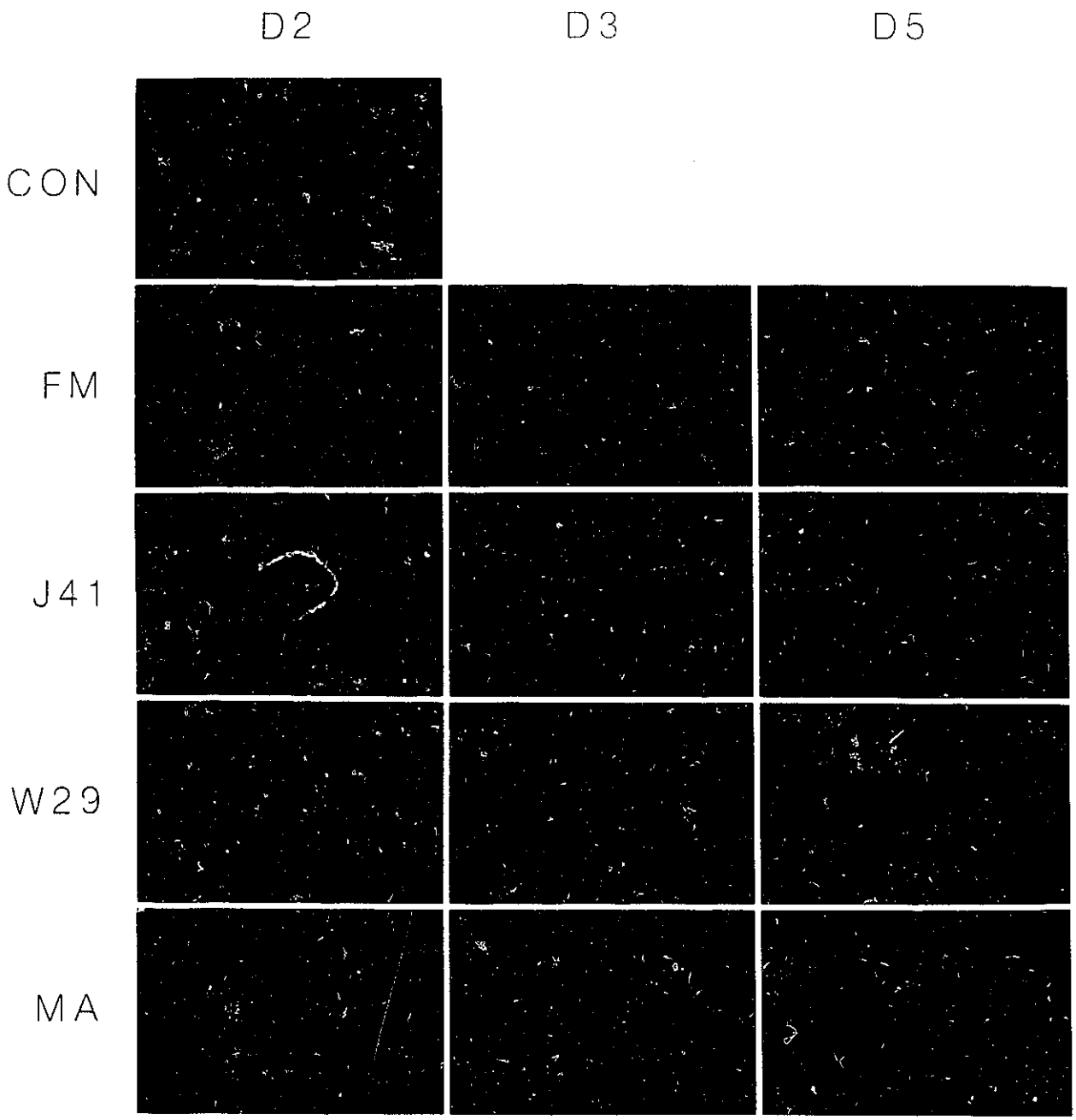
D2
D3
D5
CON
FM
J41
W29
MA

viruses. In practice, while looking under the microscope, the difference is shockingly apparent. MA has by far the most antigen positive cells, with whole fields filled with fluorescent cells. An interesting detail that arises from this composite is found in the photographs from J41 day 2 and MA day 5. These both show heavily stained cells right next to an area of negative cells. In the case of J41 this is in an airway where half of the cells are affected and half are not. For MA these are two separate lobes of lung with one nearly entirely infected and right next to it is uninfected lung. This may be an indication of how the virus spreads, possibly with gravity via airways. It also indicates that spread in bronchioles may be cell to cell with limited spread through the mucous layer.

A visual count of the number of fluorescent cells in the various frozen sections for the different viruses is presented in Figure 18. The sections were assessed "blindly" in that the identity of the infecting virus was masked. As described, the number of antigen positive cells steadily increases with the passage of time. There are approximately half the number of positive cells on day 3 compared to day 5. MA affects the greater number of cells and that it is difficult to distinguish between the reassortants of hemagglutinin (J41) and hemagglutinin and matrix genes (W29) and the FM parental where viral antigen positive cells are concerned. Although the numbers from FA staining of frozen

Figure 18: Fluorescent Cell Counts From FITC Labelled Frozen Sections

Bars on the figure are the average of three replicate experiments per virus, where 100 to 200 fields on each lung section were counted for fluorescent cells. The error bars are ± 1 standard deviation.
Control - open box
FM - diagonal up to the right
J41 - diagonal down to the right
W29 - crosshatched box
FM-MA - horizontal lines

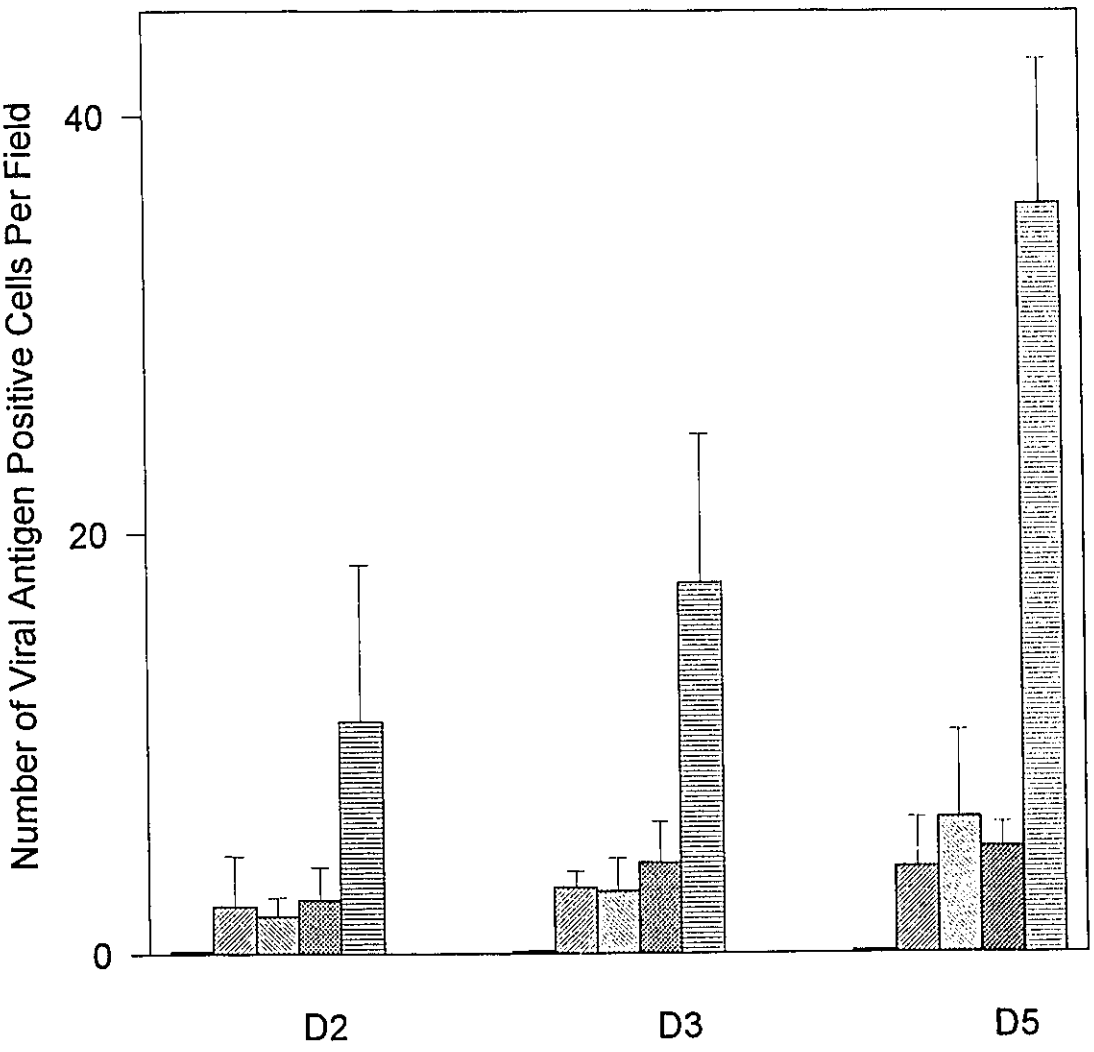
Number of Viral Antigen Positive Cells Per Field
40
20
0
D2
D3
D5

sections did not bear it out, it seemed as though there were more differences between the viruses than could be distinguished from amongst the variability of the samples. This lead to quantitative work in flow cytometry.

Flow Cytometry

Before continuing, a description of the cytometer and the settings will be provided. The cytometer is a Coulter Epics XL-MCL having an argon laser exciting at 488 nm and filters for detecting at 525, 575 and 620 ± 10 nm as well as the far red wavelengths so FITC, PE and PI could be used simultaneously. The colour compensation required for using these three fluorchromes was adjusted in the following order with single stained lung samples: Fl2(PE)-Fl1(FITC), Fl1-Fl2, Fl3(PI)-Fl2 then all dead cells (brightly positive for PI) were gated out so that the Fl2-Fl3 compensation was not excessive (Otten and Yokoyama, 1992). This resulted in 25% compensation for Fl2-Fl1, 15% for Fl2-Fl3 and 35% for Fl3-Fl2. The cytometer was detecting on a log scale for all parameters and the discriminator was set at the lowest possible setting of 1. The software used for analyzing the listmode data collected was Epics Elite also from Coulter. The cursor for gating out dead cells stained with PI was set one log unit from the origin in a Fl3 vs count histogram. Percentages of antigen positive cells were arrived at by also setting cursors in the quad stats function to 1 log unit each from the origin on a plot of Fl1 vs Fl2. Final values

were reached by subtracting the background from the test sample cells. The background consisted of lung cells labelled with pre-immune serum and the appropriate fluorochrome for each test mouse at each timepoint.

Commercially available monoclonal antibodies for the immune cells were pretested on known positive and negative cells as well as including an isotype control in a test situation. The rabbit anti-FM serum stained, collagenase treated, infected MDCK cells and the Mac-1 antibody, detected cells in collagenase treated or untreated suspension of spleen cells. Although the anti CD45 (B cells) and anti CD3 (T cells) effectively stained suspensions of spleen cells obtained by maceration through stainless steel mesh, the same cells could not be detected after subsequent collagenase treatment. Thus the former two reagents, rabbit anti-FM immune serum and Mac-1 antibody were used for flow cytometry of infected mouse lung but anti CD45 and anti CD3 were not successfully used. From all of this, Figure 19, a histogram of viral antigen positive cells was constructed. This histogram represents all cells that have labelled brightly enough with the anti influenza antibodies and secondary goat anti rabbit PE conjugate to be detected above background for PE. It is only on day 5 of infection that statistically significant differences can be seen between the segment 4 and 7 reassortant, W29 and FM-MA. Both of these have risen above the FM and J41 viruses and control to indicate that they have

Figure 19: Flow Cytometry Measurement of Viral Antigen Positive Cells

The single cell suspension was labelled with polyclonal anti-influenza antiserum then a secondary antibody conjugated with PE. The cells that are positive for viral antigen are expressed as a percentage of the total cells counted. Bars on the figure are the average of three replicate experiments for three timepoints, with error bars of ± 1 standard deviation.
Control - open box
FM - diagonal up to the right
J41 - diagonal down to the right
W29 - crosshatched box
FM-MA - horizontal lines

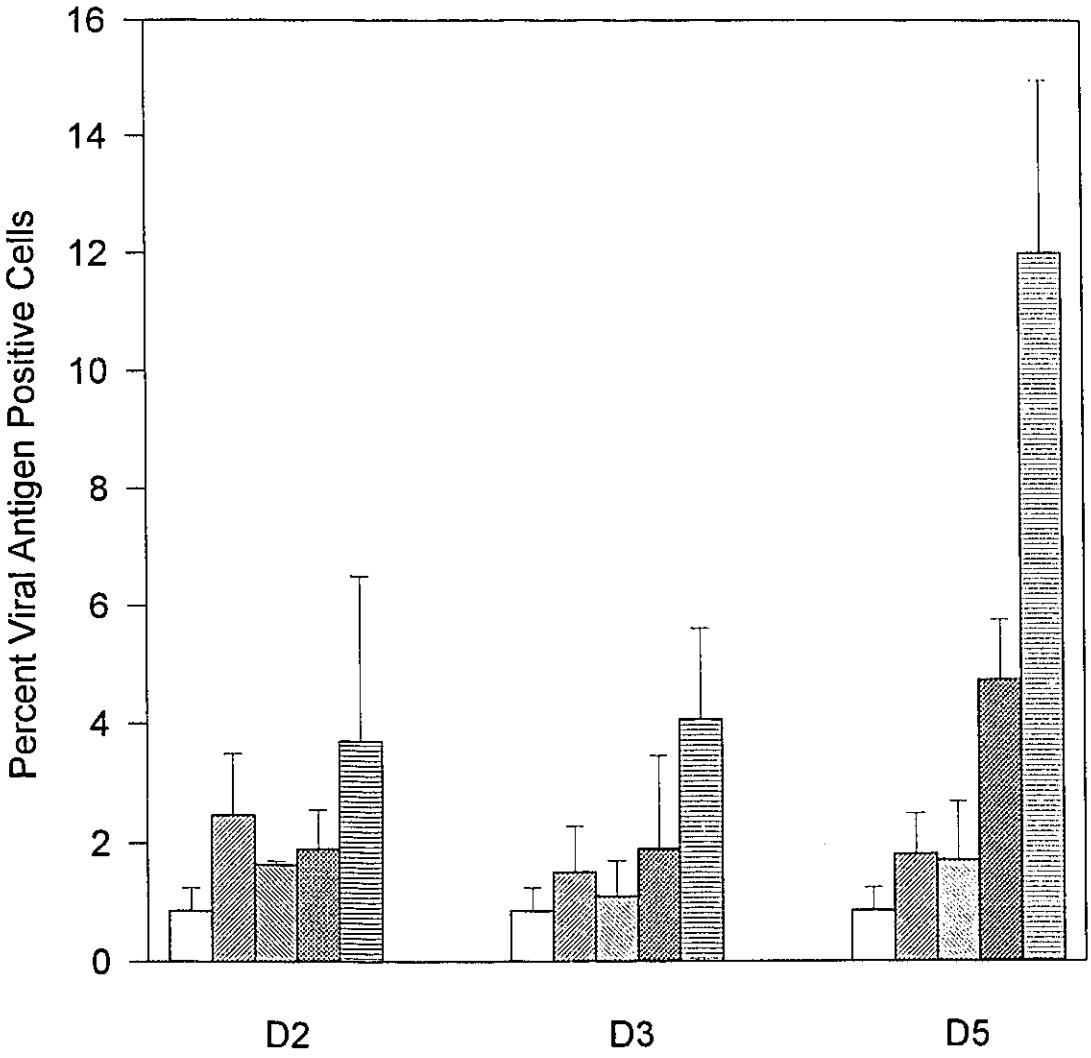
Percent Viral Antigen Positive Cells
16
14
12
10
8
6
4
2
0
D2
D3
D5

more viral antigen positive cells. MA surpasses W29 in this regard as it did in the FA staining of the frozen sections described earlier. Figure 20 shows the number of Mac-1 positive cells that carry viral antigen, so, in the cytometer these would be double stained cells with FITC and PE. Once again the difference in infected macrophage and neutrophils seen on day 5 of infection paralleled the previous figure of total infected cells. It is W29 and FM-MA again that have more viral antigen bearing Mac-1 cells with FM-MA having the most cells by far. There are more infected Mac-1 positive cells in FM-MA lungs at day 2 and 3 relative to J41 and W29 but not FM at these times due to larger standard deviation of the FM values. In Figure 21, Figures 19 and 20 are combined to give a picture of what proportion of viral antigen positive cells are made up of the Mac-1 positive immune cells. It is apparent that a large proportion of the Mac-1 cells (up to 70% for FM-MA day 5) are also positive for viral proteins and that their proportion increased with time in FM-MA and possibly W29 infected lungs. Infections with FM-MA and W29 also resulted in increases in Mac-1 positive cells.

Figure 20: Flow Cytometry Measurement of Viral Antigen Positive Cells that are also Positive for Mac-1

The single cell suspension was labelled with polyclonal anti-influenza antiserum then a secondary antibody conjugated with PE as well as a monoclonal specific for the Mac-1 cell marker that is conjugated with FITC. The cells that are positive for both viral antigen and Mac-1 are expressed as a percentage of the total cells counted. Bars on the figure are the average of three replicate experiments for three timepoints, with error bars of ± 1 standard deviation.
Control - open box
FM - diagonal up to the right
J41 - diagonal down to the right
W29 - crosshatched box
FM-MA - horizontal lines

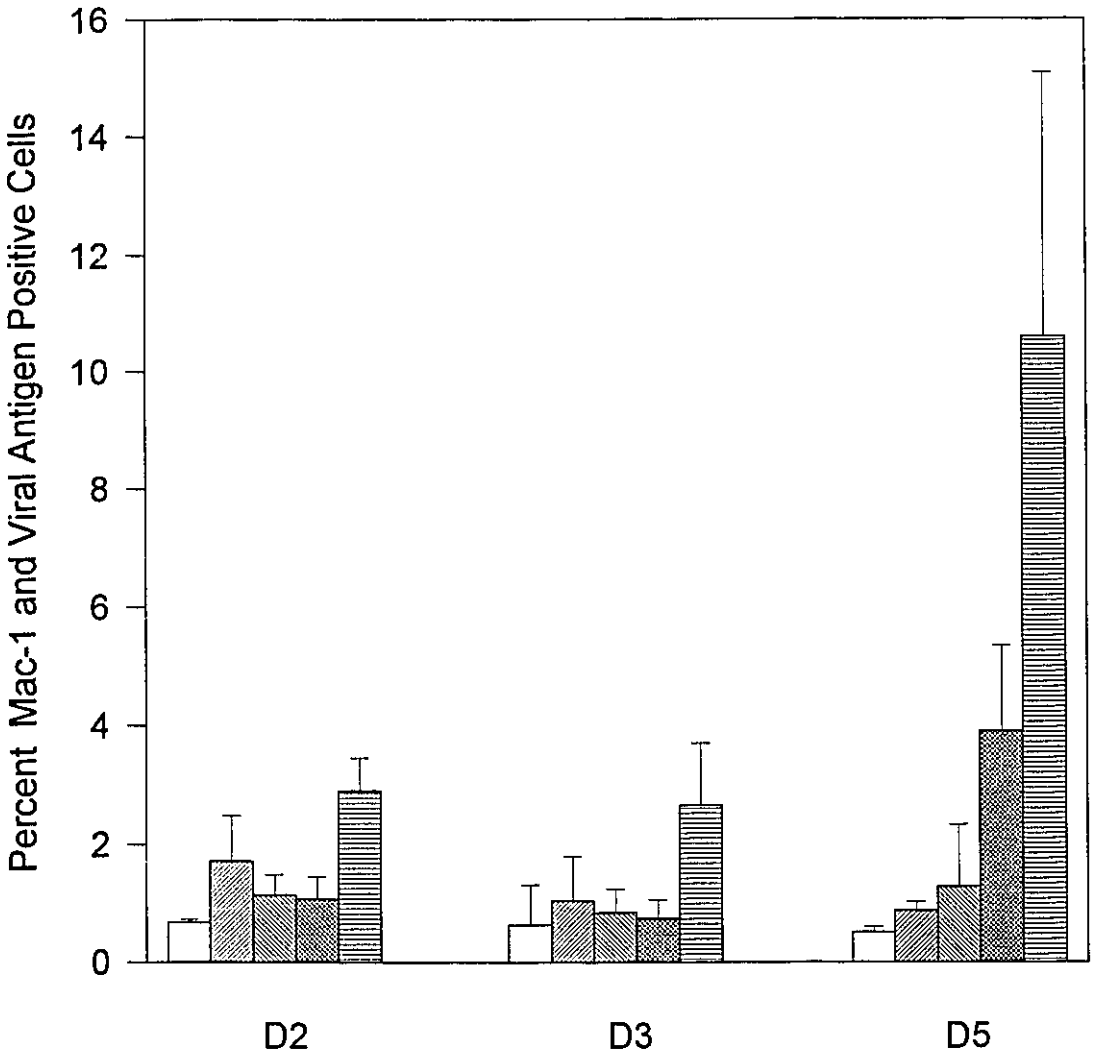
Percent Mac-1 and Viral Antigen Positive Cells
16
14
12
10
8
6
4
2
0
D2
D3
D5

Figure 21: Flow Cytometry - The Proportion of Mac-1 Positive Cells that are also Positive for Viral Antigen

The single cell suspension was labelled with polyclonal anti-influenza antiserum then a secondary antibody conjugated with PE as well as a monoclonal specific for the Mac-1 cell marker that is conjugated with FITC. The cells that are positive for Mac-1 are expressed as a percentage of the total cells counted. The cells that are positive for both viral antigen and Mac-1 are represented on the figure as checkered boxes making up the lower part of the bars. Bars on the figure are the average of three replicate experiments for three timepoints.
Control - open box
FM - diagonal up to the right
J41 - diagonal down to the right
W29 - crosshatched box
FM-MA - horizontal lines

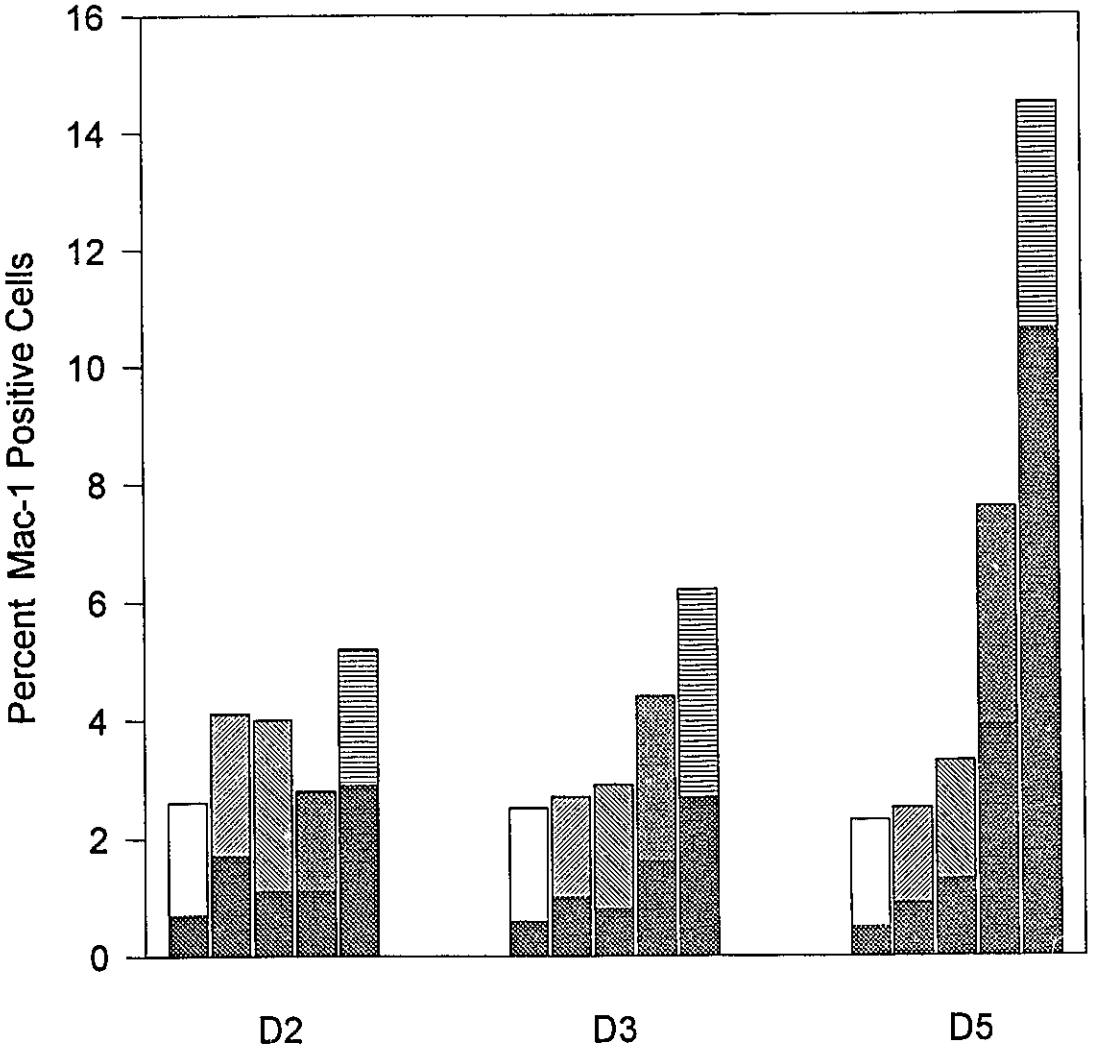
Percent Mac-1 Positive Cells
16
14
12
10
8
6
4
2
0
D2
D3
D5

DISCUSSION

The purpose of this study was to investigate the virulence determinants of influenza A virus. In work leading up to this investigation, a mouse model was developed for studying this problem. The mouse model was chosen for a variety of reasons including the fact that when human viruses are passaged in mouse lung, they will often become mouse adapted and more virulent (Hirst, 1947). In this way, there would be the original avirulent parent and a mouse adapted variant that could be compared both on a genetic level and for different functions that determine virulence. Another reason that the mouse model is a useful tool is that it mimics the most severe outcome of human influenza A viral infection, viral pneumonia (Hers et al, 1962)

In our studies, the virulence of the influenza viruses is measured in mice by the median lethal dose (LD_{50}). The FM-MA virus used in this study was previously found to have an increased LD_{50} of $10^{4.3}$ from the avirulent FM parent. In experiments also conducted previously, viral gene segments 4, 5, 7 and 8 were statistically associated with virulence. Because these segments were believed to be involved in virulence, reassortants were made with combinations of these genes from FM-MA on FM parental background. Also cDNAs of these four segments from the two viruses were cloned in order that cDNA sequencing could be carried out and the viruses compared for any changes that may have been selected on

adaptation. This is the point at which the investigation described in this thesis begins.

After sequencing the cDNA from the four segments and confirming any changes by direct genomic RNA sequencing, only three mutations were found. One of them is a change from tryptophan to glycine at amino acid position 47 of the HA2 component of the HA protein of FM and FM-MA respectively. The other two were found on the matrix protein coded for by segment 7. One of these mutations is silent, and the other changes amino acid position 139 from a threonine in FM to an alanine in FM-MA. This is a relatively low number of mutations resulting in a dramatic increase in virulence. Some authors have been troubled in the past by numerous mutations found in their viruses (Klimov et al, 1992; Cox et al, 1988). The trouble arises in attempting to discern which mutations are really important to the viral characteristics observed and which are just random in origin.

In influenza, the mutation rate is approximately one per genome per replication cycle based on the mutation rate of the NS gene (Drake, 1993). This is not to say that all genome segments have the same mutation rate. Segment 7, coding for the matrix protein, is the slowest evolving segment showing almost no accumulation of coding changes in 55 years (Webster et al, 1992). Segment 7 also codes for the M2 protein, which proportionately has more coding changes to silent changes than M1 even though they are coded for by the

same RNA strand (Ito et al, 1991). It is believed that this phenomenon is due to the fact that M2 is a viral surface protein while M1 is internal. The immune selection pressure is much higher for surface proteins and external components do not have the same structural constraints as internal components (Webster et al, 1992). HA, coded for by segment 4, is a major target of the humoral immune system and correspondingly has a higher proportion of coding to non-coding changes than internal proteins (Webster et al, 1992).

Because of the mutability of the influenza virus genome, there is always some concern that the virus will accumulate more changes during experimental manipulation so that the virus used in the beginning and the one used in the end are different. Of course, care was taken to minimize passaging the virus further and large stocks of plaque purified virus were prepared in aliquots so that the same starting material was used for all experiments. Also, all of the parental and reassortant virus strains were checked by sequencing the cDNA produced by PCR before and after passage in MDCK cells and in egg allantoic cavities to ensure that the mutations detected for virulence were stable. For a summary of this work please refer to Appendix III. In addition, the NCS proteolysis of HA2 confirmed that the HA mutation at the tryptophan is present as indicated by a difference in the pattern of the resulting peptide fragments.

Mutation at amino acid 47 of HA2 has been observed for

amantadine resistant mutants (Daniels et al, 1985). Strains of an H3N2 virus and an H7N1 virus with this amino acid mutated have both been noted for their change in the optimum pH of fusion (Wiley and Skehel, 1987). Other amantadine resistant mutants with altered HAs have also had an effect on the pH of fusion optima by as much as 0.7 pH units (Steinhauer et al, 1991; Doms et al, 1986). The importance of this pH optimum relates to the activity of the HA inside of the host cell endosome. Once the pH in the endosome is reduced sufficiently, the HA undergoes an irreversible conformational change that mediates fusion of the viral and endosomal membranes so that the viral contents may be released into the host cell cytoplasm. With FM-MA there is a 0.2 pH unit drop in the optimum pH compared to FM, from 5.7 to 5.5. What this means in terms of virulence to the host is difficult to establish. There are two points in viral replication where the pH optimum of the HA may be important.

Firstly, when the virus fuses membranes in the late endosome, the pH optimum must be such that the HA is activated by the pH in the endosome. This would not tend to be a problem in that the pH of the endosome and lysosome are estimated to be between 4.5 and 5.0 while the optimal pH of fusion for most HAs is between 5.0 and 6.2 (Beyer et al, 1986; Doms et al, 1986). Even at the upper limit of the endosome range and the lower limit of the HA fusion conformation, the pH would be sufficient to release viral

contents into the cytoplasm through fusion. The M2 ion channels that allow H+ from the acidic endosome into the virion in order to loosen the M1 from the RNP so that replication can continue are also activated by a pH of 5.0 to 6.0 so, the endosome is sufficiently acidic for this mechanism as well (Pinto et al, 1992). The only situation in which the endosome pH may not be sufficient to activate membrane fusion and uncoating is in the presence of high concentrations of the anti-influenza drug amantadine. When it is used, the endosomal pH may increase to 5.5 and as a result, only the viruses with the higher pH optima will function in fusion (Beyer et al, 1986). This would also be important in viral M1 acidification in that amantadine targets M2 protein to block the channel (Steinhauer et al, 1991).

The second place where the pH at which HA undergoes its conformational change becomes important is in the processing of newly made HA. As indicated in the introduction, the HA protein is a glycoprotein and undergoes the usual glycoprocessing from the RER to the Golgi complex and then to the host cell membrane. In the Golgi, the pH can be between 5.0 and 6.0 with the pH of the Golgi of MDCK cells being approximately 6.0 (Grambas and Hay, 1992). In order for the HA to be produced without being irreversibly inactivated before viral assembly, the pH in the Golgi must be elevated higher than the HA's pH optimum. Again the M2 ion channel

has a role in regulating the pH. It functions in trans Golgi stage of HA production whereby it is thought to insert itself in the membrane of the Golgi and allow H+ to leave the compartment, effectively raising the pH to protect the HA (Grambas et al, 1992). In the case of the FM parental, much of the HA reaching the cell surface would be inactivated if the M2 did not elevate the pH higher than 5.6.

It is apparent that M2 and HA are closely tied in viral reproduction and it has been suggested that the two should have some complementarity. If the M2 is especially efficient at increasing the pH, the HA doesn't need to be as acid stable. Grambas et al (1992) have noted that reassortment of HA and M genes in viruses that differ widely in their pH of fusion are not found. They have also noted that even a pH optimum drop of 0.2 units can enhance viral viability when M2 is mutated so that it is less efficient. In the present study, the 0.2 pH unit drop in the mouse adapted virus might reflect an increased resistance of the HA to acidic deactivation in the trans Golgi.

In continuing with the characterization of the changes brought about by the mutation in HA2 it was discovered that the HA protein of FM was more sensitive to trypsin cleavage than FM-MA. Trypsin cleavage in FM results in not only HA1 and HA2 but also another smaller product. The ease of the cleavage of HA0 into HA1 and HA2 has been implicated in virulence for chickens in influenza infection (Bosch et al,

1981). Rott et al (1984) adapted A/FM/1/47 to MDCK cells and found that the HA was endogenously cleaved. This has not been the case with the mouse adapted A/FM/1/47 used in this study. Trypsin was still required to cleave the HA so that it could subsequently undergo its fusion conformational change. The cleavability of the HA in avian influenza viruses is dependent on the sequence of amino acids that join the two subunits (Bosch et al, 1981). In this study there is only one mutation in the HA so it must be responsible for the altered pattern of cleavage. Since it is known that single amino acid substitutions near the fusion peptide can alter the globular domains of HA, it seems possible that the mutation at HA2 47 could result in a conformation change in HA (Yewdell et al, 1993). Perhaps conformation plays a role in cleavage of the protein. It is not possible to determine the meaning of this in terms of virulence for the mouse adapted virus in mouse lung. It is still unknown why some viral HAs are endogenously cleaved and why some require cleavage outside of the host cell. The protease that carries out this cleavage and its normal function within the host is also uncertain, but some researchers have found a protease produced by the Clara cells in the lung that can activate influenza virus particles (Kido et al, 1993).

As for other functions that the mutation found in HA may be having in the pathogenicity of the mouse adapted virus, altered receptor binding remains untested. Perhaps when Raut

(1975) found that his mouse adapted virus had an increased ability to infect alveolar cells it was receptor binding that was important. In a small droplet infection, the infection doesn't need to descend from the upper respiratory tract to the lower respiratory tract, but can infect alveolar cells directly and cause viral pneumonia (Hers et al, 1962). So, if the virus can infect a wider variety of cells or a specific cell type with a critical function, it would have an impact on the overall virulence of the virus.

In the remaining experiments that were conducted to find a biological role for mutated segments, mutant HA reassortants showed no changes compared with FM parental in replication kinetics, immune cell recruitment and extent of lung infection as determined by flow cytometry. From the preceding discussion it is obvious that HA is altered both in fusion characteristics and cleavage properties and from LD_{50} studies with an HA reassortant, HA is contributing to the virulence and produces increased bronchopneumonia, but the function that controls increased virulence for this mutated gene has not yet been elucidated.

As described in the introduction, one of the functions of the matrix protein encoded for by segment 7 is to lead the viral RNP from the nucleus to the cell membrane in viral assembly (Enami et al, 1993). There is also a critical step in uncoating during viral entry where M1 must be dissociated from the RNP after acidification in the endosome so that the

RNP may go to the nucleus for replication (Martin and Helenius, 1991). In figure 3 of the results, a map of functional sites on segment 7 has been included with the location of the mutations on FM and FM-MA. This map was compiled from data learned in antitranscriptase inhibition experiments, where the binding of certain monoclonal antibodies to M1 prevented the shut down of transcription (Ye et al, 1989). The coding mutation on FM-MA M1 protein is located in the middle of an RNA binding area with antitranscriptase activity (Herlocher et al, 1992). In theory, if binding is looser or more susceptible to the low pH dissociation in the endosome, uncoating may be enhanced resulting in an improved rate of infection. Alternatively, transcription could last longer because M1 is not binding the RNP so actively in the nucleus to transport it out. In this way more viral particles could be replicated.

In the replication kinetics tested in this investigation, both in the mouse lung and in cell culture, the mouse adapted virus as well as the reassortant with segments 4 and 7 of FM-MA grew faster and to higher titer than did the segment 4 reassortant or the FM parental. It was unfortunate that a reassortant with the segment 7 only from FM-MA was not available for this experiment to confirm that segment 7 is solely responsible for the increase in growth. As described previously, segment 7 mutations have been implicated with high replicating viruses (Baez et al, 1980). It is

interesting that the reassortant W29 that possesses FM-MA HA and M1 proteins, replicates as well as FM-MA but from Table 1 it is apparent that W29 is not as virulent as the mouse adapted. So, although replication may be a virulence determinant there are other mechanisms operating in the increased virulence of the FM-MA virus.

The mouse temperature studies reflect not so much the growth of virus in the lungs or the pathology produced by infection since the timing is different, but perhaps it is more the timing of the maximum immune response or interaction with inflammatory cells such as Mac-1 positive cells. Why the temperatures drop in the lethal infections is unknown, but is highly indicative of impending death.

In an attempt to find virulence determinants other than improved replicative ability, the lung pathology in mouse was studied. This was accomplished first through standard hematoxylin, phloxine and saffron (HPS) stained formalin fixed sections, then with fluorescently stained viral antigens in frozen sections. Lastly, to get a better idea of quantity and type of cell infected, flow cytometry experiments were undertaken.

Differences were seen in the amount and type of damage caused by the different viruses in the HPS stained slides. The differences were particularly apparent in the interstitial inflammation with the segment 4 and 7 reassortant and FM-MA displaying much more interstitial

involvement especially early in the infection. This interstitial pneumonia is characteristic of a purely viral pneumonia, precisely the type pneumonia that was associated with the death of otherwise healthy young adults in the 1918 pandemic.

In the immunofluorescence labelling of viral antigens on frozen sections, the differences in quantity of positive cells was much more apparent than any change in the location of infection in the lung. FM-MA has much higher levels of infected cells than the reassortants and FM even though the reassortant W29 carries both of the mouse-adapted HA and M1 proteins and has the same replicative ability as FM-MA. As mentioned before, even the two mutations found do not account for all of the increased virulence of FM-MA so another gene, as yet unknown, must also be involved in virulence. Another interesting point that arises form this experiment as well as in the following flow cytometry experiment is the spread of viral antigen. Although day two of infection has the peak viral titer, both the FA and flow cytometry show increasing numbers of cells bearing viral antigens to the end of the five day experiment. Somehow, the antigens are present on more cells without further increases in infectious virus.

Flow cytometry is a very useful technique to study the infected cells in the mouse lung because many cells could be analyzed for multiple parameters in one preparation. Since fluorescently labelled cells could be accurately counted in

a suspension of lung cells, the results should be more accurate than the counting of positive cells in frozen sections. With four detectors available to collect information, multiple stains could be used at once so that the type of cell, infected or noninfected, as well as the integrity of the cell membrane could be tested.

There are of course drawbacks to the technique as well. Currently, most of the applications and protocols are for peripheral blood samples. Monoclonal antibodies, apart from those that recognize the immune cell markers, are not so readily available for other cell types such as those that make up the lungs.

In cytometry, the aim is to produce a single cell suspension for analysis. The enzymatic digestion and mechanical disaggregation of connective tissue used in producing single cells from a lung leads to cell damage. Severely degenerating cells do not stain specifically with fluorochrome conjugated antibodies and are likely to pick up the stain nonspecifically even with normal serum present as a blocking agent (Hers et al, 1962; Holmes, 1992). Thus, damaged cells were detected by propidium iodide staining and excluded from analysis. Influenza virus infection itself also causes cell damage so the cells that are harvested and remain intact may not be completely accurate representatives of those found in the infected lung. It is possible that cells in advanced stages of infection are permeable to

propidium iodide and thus excluded from analysis since just before running the samples in the cytometer, propidium iodide is used to stain those cells whose membrane is not longer intact. In order to avoid problems with overlapping emission spectra from PI and PE used to stain for viral antigens, all cells brightly positive for PI are excluded from the data collected (Otten and Yokoyama, 1992). Another method for removing dead cells from the samples actually involves removing the cells by centrifugation or density gradients. We were unsuccessful in removing dead cells by density gradient centrifugation of lung cells possibly due to the widely varying size, shape and condition of the cells in suspension. The details of these experiments are described in Appendix V.

Having recounted all of the drawbacks to flow cytometry it still proved to be a valuable tool in this investigation. The results confirmed what had been seen in the previous pathology studies and added to the evidence that the segment 4 and 7 reassortant also has an advantage in mouse lung infection along with FM-MA. Whether this is due solely to the increased replication ability of some other factor is not yet known. Infection of immune cells (double stained cells) was of interest because there is some indication that the immune system has a dual role in an influenza infection, both as the means by which the virus is eradicated and as a cause of pathology. It is unfortunate that the monoclonal

antibodies specific for T cells and for B cells gave results too inconsistent to be interpreted. The use of collagenase on the cells appears to strip the CD3 and CD45 antigens from them as was observed in conroel experiments conducted on splenocytes It is also unfortunate that the monoclonal anti HA antibodies that were conjugated to biotin and detected with streptavidin-FITC gave a weak signal because monoclonal antibodies are often preferred for use in flow cytometry since they tend to cause less background staining. In the end, polyclonal serum was used for viral antigen detection. Perhaps avidin-phycoerythrin conjugation of the HA monoclonal antibody would have given stronger staining, because PE is known to be better than FITC in its signal to noise ratio (Parks et al, 1989). Macrophages and neutrophils, detected by the Mac-1 monoclonal, are important in influenza infection in that they phagocytose infected cell debris and provide cytokines by which antigen specific cells of the immune system may be activated. If these phagocytes should become infected they may fail to perform their function in which case the infection would increase in severity or conversely, they might become excessively activated and unregulated, resulting in immune autotoxicity pathology. If the macrophages were productively infected, they could be involved in enhanced spread of infection especially in the alveoli where they usually represent the major source of protection. Future work need to involve a detailed analysis

of the effect of these viruses on components of the cell mediated immune response.

Conclusions

In attempting to find virulence determinants in a mouse adapted influenza A virus:

1) Two coding mutations were found when compared to the original parent; one in segment 4 HA at amino acid 47 of HA2 and one in segment 7, M1 protein at amino acid 139.

2) The segment 4 mutation results in a change of the fusion pH optimum of the HA and also its cleavage by trypsin.

3) The only biological difference that was seen in this investigation associated with segment 4 was an increased late bronchopneumonia compared to FM. Changes were not observed with regard to viral replication kinetics or immune cell recruitment.

4) The segment 7 mutation studied using a reassortant virus with segments 4 and 7 from FM-MA of an FM background resulted in increased replication (both rate and extent), increased interstitial pneumonia and greater recruitment of macrophages and neutrophils.

5) Although these mutations represent $10^{3.4}$ of a $10^{4.3}$ increase in virulence it was apparent that another gene(s) must be involved in making up the difference.

REFERENCES

Aitken, M., M. Villalon, P. Verdugo and M. Nameroff. 1991. Enrichment of subpopulations of respiratory epithelial cells using flow cytometry. Am. J. Respir. Cell. Mol. Biol. 4: 174-178.

Almond, J. 1977. A single gene determines the host range of influenza virus. Nature. 270: 617-618.

Anderson, P. 1991. Factors promoting pathogenicity of influenza virus. Sem. Respir. Infect. 6(1): 3-10.

Baez, M., P. Palese and E. Kilbourne. 1980. Gene composition of high-yielding influenza vaccine strains obtained by recombination. J. Infect. Dis. 141(3): 362-369.

Bender, A., U. Amann, R. Jager, M. Nain and D. Gemsa. 1993. Effect of granulocyte/macrophage colony-stimulating factor on human monocytes infected with influenza a virus. J. Immunol. 151: 5416-5424.

Beyer, W., R. Ruigrok, H. van Driel and N. Masurel. 1986. Influenza virus strains with a fusion threshold of pH 5.5 or lower are inhibited by amantadine. Arch. Virol. 90: 173-181.

Bosch, F., W. Garten, H. Klenk and R. Rott. 1981. Proteolytic cleavage of influenza virus hemagglutinins: primary structure of the connecting peptide between HA1 and HA2 determines proteolytic cleavability and pathogenicity of avian influenza viruses. Virol. 113: 725-735.

Brown, E. 1981. *Vesiculovirus: comparisons of protein structure and studies of the abnormal N protein of the vesicular stomatitis New Jersey D_1 temperature-sensitive mutant*. Ph.D Thesis. McMaster University.

Brown, E. 1990. Increased virulence of a mouse-adapted variant of influenza A/FM/1/47 virus is controlled by mutations in genome segments 4, 5, 7 and 8. J. Virol. 64(9): 4523-4533.

Carr, C. and P. Kim. 1993. A spring-loaded mechanism for the conformational change of influenza hemagglutinin. Cell. 73: 823-832.

Collier, R. 1974. *The plague of the Spanish lady: the influenza pandemic of 1918-1919*. The Murray Printing Co., Forge Village, Mass. pp. 304-309.

Couch, R. 1993. Advances in influenza virus vaccine research. Ann. NY Acad. Sci. 685: 803-812.

Couciero, J., J. Paulson and L. Baum. 1993. Influenza virus strains selectively recognize sialyloligosaccharides on human respiratory epithelium; the role of the host cell in selection of hemagglutinin receptor specificity. Virus Res. 29: 155-165.

Cox, N., F. Kitame, A. Kendal, H. Maassab and C. Naeves. 1988. Identification of sequence changes in the cold-adapted, live attenuated influenza virus vaccine strain, A/Ann Arbor/6/60 (H2N2). Virol. 167: 554-567.

Daniels, R., J. Downie, A. Hay, M. Knossow, J. Skehel, M. Wang and D. Wiley. 1985. Fusion mutants of the influenza virus glycoprotein. Cell. 40: 431-439.

Doms, R., M. Gething, J. Henneberry, J. White and A. Helenius. 1986. Variant influenza virus hemagglutinin that induces fusion at elevated pH. J. Virol. 57(2): 603-613.

Douglas, R. 1990. Prophylaxis and treatment of influenza. New Eng. J. Med. 322(7): 443-450.

Drake, J. 1993. Rates of spontaneous mutation among RNA viruses. PNAS. 90: 4171-4175.

Enami, K., Y. Qiao, R. Fukuda and M. Enami. 1993. An influenza virus temperature-sensitive mutant defective in the nuclear-cytoplasmic transport of the negative sense viral RNAs. Virol. 194: 822-827.

Enami, K., T. Sato, S. Nakada and M. Enami. 1994. Influenza virus NS1 protein stimulates translation of the M1 protein. J. Virol. 68(3): 1432-1437.

Geliebter, J. 1987. Dideoxynucleotide sequencing of RNA and uncloned cDNA. Focus. 9(1): 5-8.

Gerhard, W., J. Yewdell, M. Frankel and R. Webster. 1981. Antigenic structure of influenza virus hemagglutinin defined by hybridoma antibodies. Nature. 290: 713-717.

Grambas, S., M. Bennett and A. Hay. 1992. Influence of amantadine resistance mutations on the pH regulatory function of the M2 protein of influenza a viruses. Virol. 191: 541-549.

Grambas, S. and A. Hay. 1992. Maturation of influenza a virus hemagglutinin. Estimates of the pH encountered during transport and its regulation by the M2 protein. Virol. 190: 11-18.

Harlow, E. and D. Lane. 1988. *Antibodies: a laboratory manual*. Cold Spring Harbor Laboratory, New York. pp. 298-299; 310; 341.

Hartshorn, K., A. Karnad and A. Tauber. 1990. Influenza a virus and the neutrophil: a model of natural immunity. J. Leuk. Biol. 47: 176-186.

Hatada, E. and R. Fukuda. 1992. Binding of influenza a virus NS1 protein to dsDNA in vitro. J. Gen. Virol. 73: 3325-3329.

Helenius, A. 1992. Unpacking the incoming influenza virus. Cell. 69: 557-578.

Hennett, T., H. Ziltener, K. Frei and E. Peterhans. 1992. A kinetic study of immune mediators in the lungs of mice infected with influenza a virus. J. Immunol. 149: 932-939.

Herlocher, L., D. Bucher and R. Webster. 1992. Host range determination and functional mapping of the nucleoprotein and matrix genes of influenza viruses using monoclonal antibodies. Virus Res. 22: 281-293.

Herlocher, L., H. Maassab and R. Webster. 1993. Molecular and biologically changes in the cold adapted "master strain" A/AA/6/60 (H2N2) influenza virus.

Hers, J., J. Mulder, N. Masurel and L. Kuip. 1962. Studies on the pathogenesis of influenza virus pneumonia in mice. J. Path. Bacteriol. 83: 207-217.

Higa, H., G. Rogers and J. Paulson. 1985. Influenza virus hemagglutinins differentiate between receptor determinants bearing N-acetyl, N-glycollyl, and N,O-diacetylneuraminic acids. Virol. 114: 279-282.

Hirst, G. 1947. Studies on the mechanism of adaption of influenza virus to mice. J. Exp. Med. 86: 357-366.

Holmes, K. and B. Fowlkes. 1992. Preparation of cells and reagents for flow cytometry. In *Current protocols in immunology*. Edited by J. Coligan, A. Kruisbeek, D. Margulies, E. Shevach and W. Strober. Greene Publishing Associates and Wiley-Intersciences, Toronto. pp. 5.3.1-5.3.8.

Holsinger, L., D. Nichani, L. Pinto and R. Lamb. 1994. Influenza a virus M2 ion channel protein: a structure-function analysis. J. Virol. 68(3): 1551-1563.

Ito, T., O. Gorman, Y. Kawaoka, W. Bean and R. Webster. 1991. Evolutionary analysis of the influenza a virus M gene with comparison of the M1 and M2 proteins. J. Virol. 65(10): 5491-5498.

Johnston, R. 1988. Monocytes and macrophages. New Eng. J. Med. 318(12): 747-752.

Katz, J. and J. Robertson. 1992. WHO-NIH meeting on host cell selection of influenza virus variants. Vaccine. 10: 723-725.

Katz, J. and R. Webster. 1992. Amino acid sequence identity between the HA1 of influenza a (H3N2) viruses grown in mammalian and primary chick kidney cells. J. Gen. Virol. 73: 1159-1165.

Katze, M. and R. Krug. 1990. Translational control in influenza virus infected cells. Enzyme. 44: 265-277.

Kees, U. and P. Krammer. 1984. Most influenza virus specific memory cytotoxic T lymphocytes react with antigenic epitopes associated with internal virus determinants. J. Exp. Med. 159: 365-377.

Kemble, G., T. Danieli and J. White. 1994. Lipid anchored influenza hemagglutinin promotes hemifusion, not complete fusion. Cell. 76: 383-391.

Kido, H., K. Sakai, Y. Kashiro and M. Tashiro. 1993. Pulmonary surfactant is a potential endogenous inhibitor of proteolytic activation of Sendai virus and influenza a virus. FEBS Letters. 322(2): 115-119.

Kilbourne, E. 1987. *Influenza*. Plenum Press, New York. pp. 3-22; 72; 57-205.

Kingsbury, D. 1990. Orthomyxoviridae and their replication. In *Fields Virology*. 2nd ed. Edited by B. Fields, D. Knipe, R. Chanock, M. Hirsh, J. Melnick, T. Monath and B. Roizman. Raven Press, New York. pp. 1075-1090.

Klimov, A., N. Cox, W. Yotov, E. Rocha, G. Alexandrova and A. Kendal. 1992. Sequence changes in live attenuated, cold-adapted variants of influenza A/Leningrad/134/57 (H2N2) virus. Virol. 186: 795-797.

Krug, R., F. Alonso-Kaplan, I. Julkman and M. Katze. 1989. Expression and replication of the influenza virus. In *The influenza viruses*. Edited by R. Krug. Plenum Press, New York. pp. 89-142.

Laemmli, U. 1970. Cleavage of structural proteins during the assembly of the head of bacteriophage T4. Nature. 227: 680-685.

Lamb, R. 1989. Genes and proteins of influenza viruses. In *The influenza viruses*. Edited by R. Krug. Plenum Press, New York. pp. 1-67.

Larson, E., J. Dominick, A. Rowberg and G. Higbee. 1976. Influenza population dynamics in the respiratory tract of experimentally infected mice. Infect. Immun. 13(2): 438-447.

Li, S., J. Schulman, S. Itamura and P. Palese. 1993. Glycosylation of neuraminidase determines the neurovirulence of influenza A/WSN/33 virus. J. Virol. 67(11): 6667-6673.

Luytjes, W., M. Krystal, M. Enami, J. Parvin and P. Palese. 1989. Amplification, expression and packaging of a foreign gene by influenza virus. Cell. 59: 1107-1113.

Marsh, M. and A. Helenius. 1989. Virus entry into animal cells. Adv. Virus Res. 36: 107-138.

Martin, K. and A. Helenius. 1991. Nuclear transport of influenza virus ribonucleoproteins: the viral matrix protein (M1) promotes export and inhibits import. Cell. 67: 117-130.

Mims, C. 1976. The pathogenesis of influenza. In *Influenza: virus vaccines and strategy*. Edited by P. Selby. Academic Press, New York. pp. 95-108.

Mims, C. 1987. *The pathogenesis of infectious disease*. Academic Press, Toronto. p.270.

Monto, A. and N. Arden. 1992. Implications of viral resistance to amantadine in control of influenza a. Clin. Infect. Dis. 15: 362-367.

Otten, G. and W. Yokoyama. 1992. Flow cytometry analysis using the Becton-Dickinson FACScan. In *Current protocols in immunology*. Edited by J. Coligan, A. Kruisbeek, D. Margulies, E. Shevach and W. Strober. Greene Publishing Associates and Wiley-Intersciences, Toronto. pp. 5.4.1- 5.4.13.

Palache, A., W. Beyer, G. Luchters, R. Volker, M. Sprenger and N. Masurel. 1993. Influenza vaccines: the effect of vaccine dose on antibody response in primed populations during the ongoing interpandemic period. A review of the literature. Vaccine. 11(9): 892-908.

Parks, D., L. Herzenberg and L. Herzenberg. 1989. Flow cytometry and fluorescence activated cell sorting. In *Fundamental Immunology*. 2nd ed. Edited by W. Paul. Raven Press, New York. pp. 781-818.

Peterhans, E., T. Jungi and R. Stocker. 1988. Autotoxicity and reactive oxygen in viral disease. UCLA Symp. Mol. Cell. Biol. 82: 543-562.

Pinto, L., L. Hosinger and R. Lamb. 1992. Influenza virus M2 protein has ion channel activity. Cell. 69: 517-528.

Raut, S., J. Hurd, R. Cureton, G. Blandford and R. Heath. 1975. The pathogenesis of infections of the mouse caused by virulent and avirulent variants of influenza virus. J. Med. Microbiol. 8: 127-136.

Ray, C. 1990. Respiratory viruses. In *Medical microbiology*. 2nd ed. Edited by J. Sherris. Elsevier Science Publishing Co. Inc., New York. pp. 499-507.

Richardson, J and R. Akkina. 1991. NS2 protein of influenza virus is found in purified virus and phosphorylated in infected cells. Arch. Virol. 116: 69-80.

Rott, R., M. Orlich, H. Klenk, M. Wang, J. Skehel and D. Wiley. 1984. Studies on the adaption of influenza viruses to MDCK cells. EMBO J. 3(13): 3329-3332.

Sanger, F., S. Nicklen and A. Coulson. 1977. DNA sequencing with chain terminating inhibitors. PNAS. 74(12): 5463-5467.

Scholtissek, C., R. Rott, M. Orlich, E. Harms and W. Rohde. 1977. Correlation of pathogenicity and gene constellation of an influenza virus (fowl plague) 1. Exchange of a single gene. Virol. 81: 74-80.

Shechter, Y., A. Patchornik and Y. Burstein. 1976. Selective chemical cleavage of tryptophanyl peptide bonds by oxidative chlorination with N-chlorosuccinimide. Biochem. 15(23): 5071-5075.

Small, P. 1990. Influenza: pathogenesis and host defense. Hospital Practice. 25: 51-62.

Smeenk, C. and E. Brown. 1994. The influenza virus variant A/FM/1/47-MA possesses single amino acid replacements in the hemagglutinin, controlling virulence, and in the matrix protein controlling virulence as well as growth. J. Virol. 68(1): 530-534.

Steinhauer, D., S. Wharton, J. Skehel, D. Wiley and A. Hay. 1991. Amantadine selection of a mutant influenza virus containing an acid-stable hemagglutinin glycoprotein: evidence for virus specific regulation of the pH of glycoprotein transport vesicles. PNAS. 88: 11525-11529.

Stein-Streilein, J., M. Bennett, D. Mann and V. Kumar. 1983. Natural killer cells in mouse lung: surface phenotype, target preference, and response to local influenza virus infection. J. Immunol. 131(6): 2699-2704.

Stuart-Harris, C., G. Schild and J. Oxford. 1985. *Influenza, the virus and the disease*. 2nd ed. Edward Arnold Ltd. London. pp. 46-54; 118-134.

Sugiura, A. and M. Ueda. 1980. Neurovirulence of influenza virus in mice 1. Neurovirulence of recombinants between virulent and avirulent virus strains. Virol. 101: 440-449.

Sweet, C. and H. Smith. 1980. Pathogenicity of influenza virus. Microbiol. Rev. 44(2): 303-330.

Tait, A., B. Davidson, K. Johnson, D. Remick and P. Knight. 1993. Halothane inhibits the intraalveolar recruitment of neutrophils, lymphocytes and macrophages in response to influenza virus infection in mice. Anesth. Analg. 76: 1106-1113.

Takeuchi, K. and R. Lamb. 1994. Influenza virus M2 protein ion channel activity stabilizes the native form of fowl plague virus hemagglutinin during intracellular transport. J. Virol. 68(2): 911-919.

Tate, R. and J. Repine. 1983. Neutrophils and adult respiratory disease syndrome. Am. Rev. Resp. Dis. 128: 552-559.

Taylor, G. 1993. A rational attack on influenza. Nature. 363: 401-402.

vonItzstein, M., W. Wu, G. Kok, M. Pegg, J. Dyason, B. Jin, T. VanPhan, M. Smythe, H. White, S. Oliver, P. Coleman, J. Varghese, M. Ryan, J. Woods, R. Bethell, V. Hotham, J. Cameron and C. Penn. 1993. Rational design of potent sialidase-based inhibitors of influenza virus replication. Nature. 363: 418-423.

Ward, A., A. Azad and J. McKimm-Breschkin. 1994. Identification of sequence changes in neurovirulent strains of influenza. Arch. Virol. In Press.

Webster, R., W. Bean, O. Gorman, T. Chambers and Y. Kawaoka. 1992. Evolution and ecology of influenza a viruses. Microbiol. Rev. 56(1): 152-179.

Webster, R., Y. Kawaoka and W. Bean. 1986. Molecular changes in A/Chicken/Pennsylvania/83 (H5N2) influenza virus associated with acquisition of virulence. Virol. 149: 165-173.

Webster, R. and R. Rott. 1987. Influenza virus a pathogenicity. The pivotal role of hemagglutinin. Cell. 50: 665-666.

Webster, R., S. Wright, M. Castrucci, W. Bean and Y. Kawaoka. Influenza - a model of an emerging virus disease. Intervirol. 35: 16-25.

Wiley, D. and J. Skehel. 1987. The structure and function of the hemagglutinin membrane glycoprotein of influenza virus. Ann. Rev. Biochem. 56: 365-394.

Winship, P. 1989. An improved method for directly sequencing PCR amplified material using dimethyl sulfoxide. Nucl. Acids Res. 17(3): 1266.

Wyde, P. and T. Cate. 1978. Cellular changes in lungs of mice infected with influenza virus: characterization of the cytotoxic responses. Infect. Immun. 22(2): 423-429.

Wyde, P., R. Couch, B. Mackler, T. Cate and B. Levy. 1977. Effects of low and high passage influenza virus infection in normal and nude mice. Infect. Immun. 15(1): 221-229.

Ye, Z., N. Baylor and R. Wagner. 1989. Transcription inhibition and RNA-binding domains of influenza a virus matrix protein mapped with anti-idiotypic antibodies and synthetic peptides. J. Virol. 63(9): 3586-3594.

Yewdell, J., A. Taylor, A. Yellen, A. Caton, W. Gerhard and T. Bachi. 1993. Mutations in or near the fusion peptide of the influenza virus hemagglutinin affect an antigenic site in the globular region. J. Virol. 67(2): 933-942.

APPENDIX I : SOLUTIONS

ACK Buffer

150 mM NH_4Cl
1 mM $KHCO_3$
0.1 mM disodium EDTA
adjust pH to 7.2 - 7.4 with 1N HCl
filter sterilize

Alsever's Solution

2% glucose
25 mM sodium citrate
110 mM NaCl
3.6 mM citric acid
filter sterilize

Carnoy's Fixative

3 parts methanol with 1 part acetic acid

Citrate Buffer

0.1 M citrate buffer was made by mixing 0.2 M sodium citrate with 0.2 M citric acid in varying proportions to genrate solutions with pHs between 4.9 and 6.0 in increments of 0.1. Water and NaCl were added to give final concentrations of 65 mM NaCl and 0.1 M citrate.

Fixative for Acrylamide Gels

7% acetic acid
25% methanol
the remainder is made up with water

PBS (Phosphate Buffered Saline)

8.0 mM Na_2HPO_4
2.5 mM NaH_2PO_4
145 mM NaCl
pH 7.4 sterilize by autoclaving

PCR (Polymerase Chain Reaction) Buffer

50 mM KCl
10 mM Tris-HCl pH 8.4
1.5 mM $MgCl_2$
0.01% (w/v) gelatin

RIPA (Radioimmunoprecipitation) Lysis Buffer

50 mM Tris pH 8 - 9
150 mM NaCl
1% (w/v) NP40
10% (v/v) glycerol
1 mM PMSF (added just before use)

RIPA Washing Buffer

100 mM Tris pH 8 - 9
500 mM LiCl
1% (v/v) 2-mercaptoethanol

2X Sample Buffer

125 mM Tris-HCl pH 6.8
20% (v/v) glycerol
4% (v/v) sodium dodecylsulfate
10% (v/v) 2-mercaptoethanol
0.1% (w/v) bromophenol blue
dilute with water

STE Buffer

100 mM Tris-HCl pH 8.0
1 M NaCl
10 mM EDTA
sterilize by autoclaving

Tank Buffer

25 mM Tris
192 mM glycine
0.1% sodium dodecylsulfate

TBE Buffer

89 mM boric acid
89 mM Tris
20 mM EDTA
sterilize by autoclaving

TE Buffer

10 mM Tris-HCl pH 7.4
1 mM EDTA pH 8.0
sterilize by autoclaving

2YT

16 g Bacto tryptone
10 g yeast extract
5 g NaCl
water to 1L
sterilize by autoclaving

APPENDIX II : OLIGONUCLEOTIDE PRIMERS

All primers are written 5' to 3'. Unless otherwise indicated, the primers were used to sequence cDNA clones. Negative sense primers are indicated by an asterisk.

Universal:

M13F	GTT TTC CCA GTC ACG AC
*M13R	CAG GAA ACA GCT ATG ACC ATG
*Flu-T7	TAA TAC GAC TCA CTA TAA GTA GAA ACA AG for PCR amplification of seg 7 mutation only

Segment 4:

1;20	AGC AAA AGC AGG GGA AAA TA
220	ACA CTC TGT AAA CCT ACT CG
459	ACA ACA TAA CCA GAG GAG
639	GGA TCA AAA GAC CCT CTA
838	GGT ATG CTT TCG CAC TG (PCR)
1017	TTG AGG ATG GTT ACA GGA for sequencing mutation site
1257	GCT GTG GGT AAA GAA TTC
*1275	GAA TTC TTT ACC CAC AGC (PCR only)

Segment 5:

CS1B+	GGC TGA TCC AGA ACA GCT
*CS3R	GAC TTG TGA GCA ACT GAC
CS3+	AAG AGC AAT GAT GGA TCA
CS4+	GCC TAA TCA GAC CGA ACG
NP1400	GCA AGA CCA GAA GAA GTG

Segment 7:

7.5	GGT AGA TAT TGA AAG TTG

239 CGA GGA CTG CAG CGT AGA
for sequencing mutation site and for PCR

505 GTC TCA TAG GCA AAT GGT

758 GGG GTG CAG ATG CAA CG

Segment 8:

8.5 GGG TGA CAA AGA CAT AAT GG

215 GAT AGT GGA GAG GAT TCT

418 AAG CGA ATT TCA GTG TGA

653 TGG GAG ACC TCC ACT CA

APPENDIX III : STABILITY OF MUTATIONS

In the general discussion earlier, the concern about genome stability and reversion of mutations was raised. Several authors have noted that growth of the same virus on different cell types can result in selection of mutant forms of virus (Katz and Robertson, 1992). For example, the growth of mammalian viruses on MDCK (dog kidney) cells will often result in fewer changes to the virus compared to the same virus grown in eggs or chick embryo fibroblasts (Katz and Webster, 1992).

In order to establish that both the parental viruses and the reassortant viruses used in this investigation remained unchanged at our mutation sites after growth of the stock virus in eggs, their sequence was verified through direct sequencing of PCR products. There is also a shift in the M1 protein that was useful for the identification of the mutation in that segement. In Figure 22, this confirmation of the M1 protein origin is demonstrated. For M1 segments originating from the mouse adapted virus, there is a small shift down on the gel compared to M1 of FM. All of the parentals and reassortants gave consistent results for the PCR product sequencing and the M1 protein shift analysis. The presence of the FM-MA mutation on segment 4 containing reassortants (J9, J41, M13, W29, TSR17, T142, T154) was confirmed by sequencing DNA produced by RT-PCR.

Having demonstrated that the viruses used in the

Figure 22: Confirmation of M1 Origin in Reassortants

The ^{35}S-methionine labelled influenza proteins from an infected cell lysate were run on a 12.5% SDS-PAGE. Due to the matrix protein mutation, the FM-MA matrix protein runs faster under these conditions than that of FM. This allows for the easy identification and confirmation of the origin of the M1 in the reassortant viruses used. The control lane is a labelled, uninfected cell lysate. Lanes 1, 5, and 13 are cell lysates from FM-MA infection. Lanes 2, 8, and 12 are from J9 infection. The remainder of the viruses are tested individually with J41 in lane 3, FM in lane 4, M13 (a segment 4 and 7 reassortant) in lane 6, W29 in lane 7, TSR17 in lane 9, T142 (same as TSR17) in lane 10, and T154 in lane 11.


C 1 2 3 4 5 6 7 8 9 10 11 12 13
—NP
—M1

experiments contained the mutations that we wanted to study, we were curious to see if the FM parental virus would be stable after a series of deliberate passages. After passaging the virus in egg fluid three times, or on MDCK cells three times, no change was found in the segment 4 mutation site by PCR product sequencing. Since this is true, it appears that the mutation site being investigated on segment 4 is quite stable in both dog and chicken cells.

APPENDIX IV : MONOCLONAL ANTIBODY PURIFICATION AND BIOTINYLATION

The anti HA monoclonal antibodies used to precipitate the HA protein for NCS proteolysis of HA2 and the biotinylated antibody used for labelling infected cells in flow cytometry were prepared from a hybridoma cell line (Cb 13) donated by Dr. W. Gerhard (Gerhard et al, 1981).

The hybridoma cells were thawed into RPMI 1640 (Gibco) containing 10% fetal calf serum and incubated in 5% CO_2 at 37°C. After a few weeks of growth, the cells became contaminated with what was believed to be a yeast. Approximately 3 x 10^6 cells were injected into each of three Balb/c mice in order to produce MAb rich ascitic fluid and to decontaminate the hybridoma cells. The mice were primed two weeks earlier with 0.5 ml of Pristane injected intraperitoneally. Two weeks after the cell injection, the ascitic fluid from the mice was collected over a series of days. This ascitic fluid was tested in an immune precipitation to ensure that the fluid contained specific antibodies for the influenza HA protein. Figure 23 is a picture of an autoradiograph of an immune precipitation of ^{35}S-methionine labelled influenza proteins with both polyclonal and the new monoclonal antibodies. Since it appeared that the MAb was capable of selectively binding to the HA protein as it should, the ascitic fluid was purified by ammonium sulfate precipitation and the low salt protein A

Figure 23: Immunoprecipitation of Influenza Proteins

The ^{35}S-methionine labelled influenza proteins from an infected cell lysate were run on a 10% SDS-PAGE (lane 2). The proteins were also immune precipitated with either polyclonal anti-influenza antiserum (lane 1) or monoclonal anti-HA ascitic fluid from two different mice (lanes 4 and 5). Lane 3 is immuneprecipitated with culture medium from Y8-2D1 cells. These cells appear to have stopped producing anti-HA antibody.

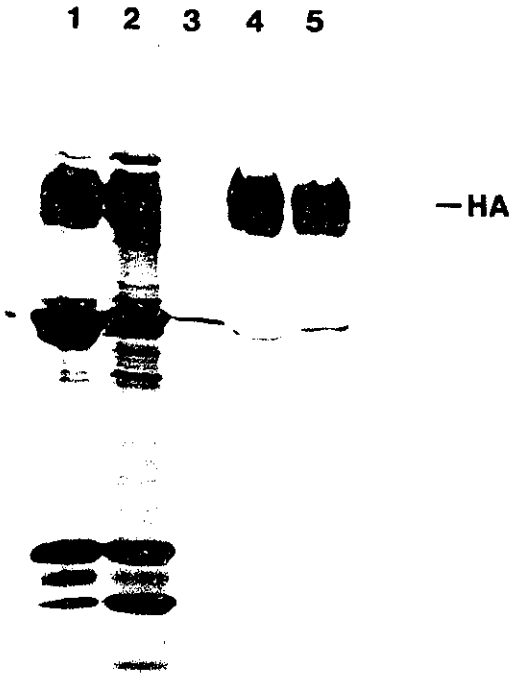
1 2 3 4 5
—HA

column methods described in Antibodies: A Laboratory Manual (Harlow and Lane, 1988). In ammonium sulfate precipitation, the ascitic fluid was mixed with 0.5 volumes of saturated ammonium sufate and allowed to incubate at 4 °C overnight. The precipitate was collected by centrifuging at 3000 g for 30 min then the precipitate was resuspended in water and dialyzed against PBS overnight. The dialysate was loaded on a 0.5 ml protein A sepharose column (packed volume) that had been washed with 1 M Tris (pH 8.0). After being loaded with antibodies, the column was then washed with ten volumes each of 100 and 10 mM Tris (pH 8.0). 100 mM glycine (pH 3.0) was used to elute the antibodies from the column into a tube containing 1 M Tris (pH 8.0) where the neutral pH could be reestablished. These antibodies were precipitated again with at least 1 volume of saturated ammonium sulfate to concentrate them, resuspended in a small amount of water and then dialyzed against PBS. The final concentration of the antibody suspension by spectrophotometry was 7.4 mg/ml. (1 OD_{280} = 0.8 mg/ml) These purified antibodies were biotinylated using N-hydroxysuccinamide biotin (Pierce) with a long spacer arm by the method also described in the book Antibodies: A Laboratory Manual with some modifications. In this method, the biotin is dissolved in DMSO to 10 mg/ml and mixed with antibodies at a ratio of 25 to 250 μg biotin/mg of antibody. We did this in three reactions using the upper limit of the range the lower limit and one intermediate. The

biotinylation occurred at room temperature for 4 hours after which, the reaction was quenched with ammonium chloride. The labelled antibodies were dialyzed against large volumes of PBS overnight. To test the efficiency of the labelling, the high, medium and low biotinylations were diluted 1 in 200 and each used to detect viral antigens on frozen sections of infected mouse lungs as previously described. Streptavidin-FITC was used in a 1 in 100 dilution in the secondary incubation step. Controls consisting of infected lung sections with pre-immune serum followed by streptavidin-FITC and streptavidin-FITC alone were used as well as normal lung sections with the biotinylated MAb and the FITC conjugate. The negative controls were all unstained and the three concentrations of biotin labelling the antibodies were all of sufficient fluorescence to warrant mixing the three preparations for use in the flow cytometry experiments. Titration of the MAb in the flow cytometry protocol resulted in the best signal to background at a 1 in 100 dilution.

APPENDIX V : FLOW CYTOMETRY

Enzymes to Make a Lung Cell Suspensions

As flow cytometry is a relatively new technique especially for non-peripheral blood samples, a method for the preparation of a single lung cell suspension had to be optimized. Other authors in related work used hyaluronidase, DNase, pronase, collagenase and trypsin for the dissociation of cells (Aitken et al, 1991; Stein-Streilein et al, 1983). Since trypsin and collagenase are common enzymes used for separating cells these were the first two tried in this investigation. They were compared for cell yields, damage to cells and for optimum labelling of viral antigens. The optimum labelling of viral antigens was tested using virus infected MDCK cells treated with either the trypsin or collagenase as well as using mouse lung. Although giving comparable results for cell yields, the trypsin damaged more of the cells in processing and made processing more difficult with clumping of samples so that collagenase was chosen as the enzyme to be used in lung cell disaggregation even though it gave slightly less fluorescent signal.

The Removal of Unwanted Cells

Upon starting flow cytometry experiments, it quickly became apparent that discriminating positive cells from negative cells relied on a low amount of background and removal of contaminating RBCs.

Much of the background in flow cytometry arises from dead cells that non-specifically soak up the stains being used. To manage the dead cells, they must either be removed from the sample before inserting the sample in the cytometer or they must be detected by the cytometer when running the sample and exclude them at that time or during analysis. The stain most commonly used for marking the dead cells for detection by the cytometer is propidium iodide because this stain only enters cells whose membranes are damaged and PI can be excited by the same wavelength laser as PE and FITC. The drawback to using PI to detect dead cells, results from the overlapping emission spectra that PE and PI share (Parks et al, 1989). So that PI doesn't give a false positive signal to the PE in a sample, its contribution to the PE signal must be compensated. Because the overlap is large, the compensation is also extensive and as a result, weak signals of PE may be missed in the detector. This is unfortunate in that it either forces the user to exclude PE from all samples so that the conflict does not arise or risk losing positive cells. Often PE is the preferred fluorochrome for use in flow cytometry because it gives a better signal to noise ratio than FITC (Parks et al, 1989). If PE is excluded from use this also eliminates the potential for staining the cells for multiple markers because substitute stains are as yet hard to find. So the best alternative to solve the dead cell problem would be to

exclude the dead cells from the sample even before it is run in the cytometer.

Apart from the high background due to dead cells, there was also the problem of contaminating cells. The irrelevant contaminating cells in our case were red blood cells that remained in the lung capillaries and those that coated the outside of the lung upon excision. In order to minimize the number of RBCs that would get into the samples, which initially was as high as 50% of cells counted, the lungs were perfused by injecting heparinized PBS into the right ventricle of the heart and allowing the returning fluid to drain from a cut in the left atrium. By this method the number of RBCs was reduced but not eliminated. Another matter to be considered in this RBC contamination problem originates from the infection of the lung itself. The more severe the infection in the lung, the more damage there is to the lung and the more blood that will leak into the tissues where perfusion will have little effect. Because of this we sought another method for the removal of RBCs.

In both the dead cell problem and the RBC contamination, a method for removing the unwanted cells is needed. In lymphocyte isolation, peripheral blood is often spun on an isotonic density gradient that separates the RBCs from the lymphcytes. The commercially available product for this is called Ficoll-Paque (Pharmacia). When this product is used on human peripheral blood, the RBCs clump together and pellet

to the bottom of the tube while the lymphocytes and monocytes cannot enter due to the density of the Ficoll-Paque. Another product that is available is Percoll (Pharmacia). Percoll has been used for many applications including the elimination of dead cells in a suspension. The advantages to using Percoll include that it is more dense than Ficoll-Paque so a larger variety of cells can be separated and its osmolarity has not been adjusted so the user can customize this for cell type or species of origin. After using these two products individually and in combination with a wide range of density layers and centrifugation speeds, no consistent results for the removal of RBCs or dead cells could be found.

An alternative to the Ficoll-Paque removal of RBCs to collect lymphocytes that is also commonly used is hypotonic shock that selectively breaks apart the RBCs. We finally chose a method using the ammonium chloride containing ACK buffer to remove the erythrocytes from contaminating our flow cytometry samples without injuring the other cells. The viability of the lung cells was tested by using the dead cell stain, PI, to see if the cells treated with the ACK buffer had lost their membrane integrity.

Having solved the problem RBC contamination, the dead cell contamination still had to be resolved. The propidium iodide staining of the cells appears to be the best alternative. Since the time when we had first used the stain, a new cytometer had been purchased and had apparently

improved in its detection of PE. A protocol was also discovered that discarded brightly PI stained cells before PE and PI are colour compensated so that PI only minimally contributes to the PE staining (Otten and Yokoyama, 1992). In a test comparing cells labelled for influenza virus proteins with polyclonal antiserum and either FITC or PE as the fluorochrome, the two performed equally as well under our final experimental conditions of colour compensation for FITC, PE and PI. From these results, it was apparent that PE could be used and the staining for more than one cell marker at once was possible.